

การเผาไหม้พาทาลิกแอนไฮไดรด์บนตัวเร่งปฏิกิริยา V_2O_5/TiO_2 ที่ได้รับการเสริมด้วย

โลหะทรานซิชันและแมกนีเซียมออกไซด์



นางสาวนลินพรรณ เจริญรอย

วิทยานิพนธ์นี้เป็นส่วนหนึ่งของการศึกษาตามหลักสูตรปริญญาวิศวกรรมศาสตรมหาบัณฑิต

สาขาวิชาวิศวกรรมเคมี ภาควิชาวิศวกรรมเคมี

คณะวิศวกรรมศาสตร์ จุฬาลงกรณ์มหาวิทยาลัย

ปีการศึกษา 2546

ISBN 974-17-5053-6

ลิขสิทธิ์ของจุฬาลงกรณ์มหาวิทยาลัย

COMBUSTION OF PHTHALIC ANHYDRIDE OVER V_2O_5/TiO_2 CATALYSTS
PROMOTED WITH TRANSITION METAL AND MgO



Miss Nalinpan Charoenruay

สถาบันวิทยบริการ
จุฬาลงกรณ์มหาวิทยาลัย

A Thesis Submitted in Partial Fulfillment of the Requirements
for the Degree of Master of Engineering in Chemical Engineering
Department of Chemical Engineering

Faculty of Engineering
Chulalongkorn University
Academic Year 2003
ISBN 974-17-5053-6

นลินพรรณ เจริญรวย : การเผาไหม้พาทาลิกแอนไฮไดรด์บนตัวเร่งปฏิกิริยา V_2O_5/TiO_2 ที่ได้รับการเสริมด้วยโลหะทรานซิชันและแมกนีเซียมออกไซด์ (COMBUSTION OF PHTHALIC ANHYDRIDE OVER V_2O_5/TiO_2 CATALYSTS PROMOTED WITH TRANSITION METAL AND MgO) อ. ที่ปรึกษา : รศ. ดร. ธราธร มงคลศิริ, 74 หน้า. ISBN 974-17-5053-6

การศึกษาสมบัติออกซิเดชันของตัวเร่งปฏิกิริยาวานาเดียมออกไซด์บนตัวรองรับไททานียัม ทั้งที่ไม่ได้รับการเสริมและที่ได้รับการเสริมด้วยโลหะทรานซิชัน (เหล็ก ทองแดง สังกะสี และ โมลิบดีนัม) และแมกนีเซียมออกไซด์ โดยใช้ปฏิกิริยาการเผาไหม้ของสารประกอบพาทาลิกแอนไฮไดรด์ ผลการทดลองแสดงให้เห็นว่าตัวเร่งปฏิกิริยาวานาเดียมออกไซด์บนตัวรองรับไททานียัม ว่องไวสำหรับปฏิกิริยาการเผาไหม้พาทาลิกแอนไฮไดรด์ เมื่อทำการเติมโลหะทรานซิชันและแมกนีเซียมออกไซด์ พบว่าทำให้การเผาไหม้ดีขึ้น แสดงให้เห็นว่าทั้งโลหะทรานซิชันและแมกนีเซียมสามารถช่วยเร่งปฏิกิริยา เนื่องจากการเติมโลหะจะช่วยเพิ่มตำแหน่งที่ว่องไวบนพื้นผิวของตัวเร่งปฏิกิริยา นอกจากนี้ การเติมแมกนีเซียมออกไซด์จะช่วยเพิ่มปริมาณของตำแหน่งที่เป็นเบสบนพื้นผิว ทำให้การดูดซับพาทาลิกแอนไฮไดรด์ดีขึ้น

สถาบันวิทยบริการ
จุฬาลงกรณ์มหาวิทยาลัย

ภาควิชา.....วิศวกรรมเคมี.....

ลายมือชื่อ..... สาขาวิชา.....วิศวกรรมเคมี.....

ลายมือชื่ออาจารย์ที่ปรึกษา..... ปีการศึกษา.....2546.....

#4570378321: MAJOR CHEMICAL ENGINEERING

KEY WORD: COMBUSTION / TRANSITION METAL OXIDE CATALYSTS / PHTHALIC ANHYDRIDE / MAGNESIUM OXIDE

NALINPAN CHAROENRUAY : COMBUSTION OF PHTHALIC ANHYDRIDE OVER V_2O_5/TiO_2 CATALYSTS PROMOTED WITH TRANSITION METAL AND MgO . THESIS ADVISOR: ASSOC.PROF. THARATHON MONGKHONSI, Ph.D. 74 pp. ISBN 974-17-5053-6.

The oxidation property of V_2O_5/TiO_2 catalyst unpromoted and promoted with transition metal (Fe, Cu, Zn and Mo) and magnesium oxide on the combustion of phthalic anhydride was investigated. The result showed that the V_2O_5/TiO_2 catalyst was not active for the combustion of phthalic anhydride. After adding both transition metal and magnesium oxide to the V_2O_5/TiO_2 catalyst, it was found that metal-V-Mg-O/ TiO_2 catalysts showed the phthalic anhydride combustion activity higher than the unpromoted V_2O_5/TiO_2 catalyst, indicating that the added transition metal and magnesium were able to catalyze the reaction. This is due to the addition of metal oxide to V_2O_5/TiO_2 catalyst would increase the active sites on the surface of catalysts. Moreover, the addition of magnesium oxide would increase the numbers of the basic sites on surface of V_2O_5/TiO_2 catalyst and increased the adsorption of phthalic anhydride, thus, provided more opportunity to react with metal.

สถาบันวิทยบริการ
จุฬาลงกรณ์มหาวิทยาลัย

DepartmentChemical Engineering..... Student's signature

Field of study... Chemical Engineering ... Advisor's signature

Academic year.....2003.....

ACKNOWLEDGEMENTS

The author would like to express her greatest gratitude and appreciation to her advisor, Associate Professor Tharathon Mongkhonsi for his invaluable guidance, providing value suggestions and his kind supervision throughout this study. In addition, she is also grateful to Associate Professor Suttichai Assabumrungrat, as the chairman, Dr. Joongjai Panpranot and Dr. Artiwan Chotipruk, who have been member of thesis committee.

Many thanks for kind suggestions and useful help to Miss Pimporn Chaicharus, Mr. Surakit Punjasamud, Miss Sujaree Kaewgun, Miss Kanda Pattamakomsan, Miss Chitlada Sakdamnusun, Miss Tananya Vongthavorn, Mr. Natthaya Kiattisirikul, Mr. Jitkarun Phongpatthanapanich, Mr. Somyod Sombatchaisak and many friends in the petrochemical laboratory who always provide the encouragement and co-operate along the thesis study.

Finally, she would like to dedicate the achievement of this work to her parents, who have always been the source of her support and encouragement.

สถาบันวิทยบริการ
จุฬาลงกรณ์มหาวิทยาลัย

CONTENTS

	PAGE
ABSTRACT (IN THAI).....	iv
ABSTRACT (IN ENGLISH).....	v
ACKNOWLEDGEMENTS.....	vi
CONTENTS.....	vii
LIST OF TABLES.....	ix
LIST OF FIGURES.....	x
CHAPTERS	
I INTRODUCTION.....	1
II LITERATURE REVIEWS.....	4
2.1 Literature reviews.....	4
2.2 Comments on previous works.....	15
III THEORY.....	16
3.1 Mechanism of oxidation reaction.....	17
3.2 Magnesium promoted transition metal oxide catalysts.....	17
3.3 Acidic and Basic Catalyst.....	18
3.4 Chemisorption at oxide surface.....	18
IV EXPERIMENTAL.....	22
4.1 Preparation of catalysts.....	23
4.2 The characterization of catalysts.....	24
4.3 The catalytic activity measurements.....	27
V RESULTS AND DISCUSSION.....	31
5.1 Catalyst characterization.....	31
5.2 Catalytic reaction.....	35
5.3 Activity and surface acidity/basicity.....	40
VI CONCLUSIONS AND RECOMMENDATIONS.....	43
6.1 Conclusions.....	43
6.2 Recommendations for future studies.....	43
REFERENCES.....	44

CONTENTS (Cont.)

	PAGE
APPENDICES	48
Appendix A. CALCULATION OF CATALYST PREPARATION	49
Appendix B. CALCULATION OF DIFFUSIONAL LIMITATION EFFECT	51
Appendix C. CALCULATION OF SPECIFIC SURFACE AREA	62
Appendix D. CALIBRATION CURVES	65
Appendix E. DATA OF EXPERIMENT	67
Appendix F. MATERIAL SAFETY DATA SHEETS	69
Appendix G. PROCEDURE AND CALCULATION OF PYRIDINE AND MALEIC ANHYDRIDE ADSORPTION	71
VITA	74

สถาบันวิทยบริการ
จุฬาลงกรณ์มหาวิทยาลัย

LIST OF TABLES

TABLES	PAGE
3.1 Classification of solids by electrical conductivity.....	18
3.2 Classification of semiconducting metal oxides.....	19
4.1 The chemicals used in this experiment.....	23
4.2 Operating conditions for gas chromatograph (GOW-MAC).....	25
4.3 Operating conditions for gas chromatograph (GC9A) for pyridine adsorption.....	26
4.4 Operating conditions for gas chromatograph (GC9A) for maleic anhydride adsorption	27
4.5 Operating conditions for gas chromatographs	29
5.1 The composition of different metal loading catalysts and BET surface area.....	31
5.2 The reference XRD patterns for transition metal oxides.....	32
5.3 The relative amounts of pyridine and maleic anhydride adsorption and the amounts of absorbed pyridine and maleic anhydride of all catalysts	41

LIST OF FIGURES

FIGURES	PAGE
4.1 Flow diagram of phthalic anhydride combustion system	28
5.1 The XRD pattern of all catalysts.....	33
5.2 The catalytic activity of copper oxide catalysts for the combustion of phthalic anhydride.....	36
5.3 The catalytic activity of iron oxide catalysts for the combustion of phthalic anhydride.....	37
5.4 The catalytic activity of zinc oxide catalysts for the combustion of phthalic anhydride.....	38
5.5 The catalytic activity of molybdenum oxide catalysts for the combustion of phthalic anhydride.....	39



สถาบันวิทยบริการ
จุฬาลงกรณ์มหาวิทยาลัย

CHAPTER I

INTRODUCTION

The oxidation of o-xylene catalysed by V_2O_5 is the major industrial process for the production of phthalic anhydride (PA). The aromatic reactant was vapourised and mixed with air in gaseous phase. The concentration of the aromatic was limited by the lower explosive limit of the gas mixture. The gas mixture then flowed to a reactor containing several thousands of catalyst tubes. The reaction proceeds at near atmospheric pressure and about 380-500°C to give almost complete conversion of o-xylene and the selectivity to phthalic anhydride of 70-75%. Catalysts contain about 7% V_2O_5 supported on TiO_2 (anatase), which in turn was carried on ceramic pellets or rings in order to increase the contact surface. The products besides phthalic anhydride include o-tolualdehyde, o-toluic acid and phthalide, together with minor amounts of maleic anhydride (MA), and the products of total combustion, carbon monoxide and carbon dioxide [Bond (1991)]. The products formed, the anhydrides, were recovered by cooling the product gas stream using a condenser.

At the condenser, it was known that the lower coolant temperature, the higher product recovery. In practice, the temperature at the condenser was limited by the concentration of water in the product gas stream. If water was allowed to condense, corrosion will occur. The effluent gas leaving the condenser, therefore, still contained traces of organic compounds including the hydrocarbon reactant and the anhydride product.

Eliminating the remaining organic compounds from the effluent gas was necessary. At present, the removal could be carried out by sending the effluent gas which still contained high oxygen concentration to a furnace. This method, however, may cause problem concerning the energy balance of the plant and NO_x forming from high temperature combustion. Catalytic combustion was an alternative. There are two catalyst families that can completely oxidize organic compounds. One is the Pt-based catalysts and the other one is the acidic metal oxide based catalysts.

The Pt-based catalysts could initiate the combustion of the organic compounds at a lower temperature than the acidic metal oxide-based catalysts, typically 100-200° C lower. But the Pt-based catalysts could not withstand prolong operation in a high oxygen concentration atmosphere. The acidic metal oxide-based catalysts worked better in the latter case.

An important nature of the acidic metal oxide catalyst was its capability to adsorbed acidic organic compounds. On the acidic surface, the acidic organic compounds was less likely to be adsorbed. The further oxidation of the acidic compound to combustion products, therefore, was low. Because of this reason, the acidic metal oxide catalyst became a selective oxidation catalyst for the production of anhydrides because it had low ability to further oxidise the anhydride product formed. On the contrary, this behavior caused problem when one has to use it as a combustion catalyst.

In order to overcome the aforementioned problem, it was proposed to dope MgO to an acidic metal oxide catalyst to enhance the adsorption of the acidic organic compounds

Previous studied discovered that magnesium oxide promoted the adsorption of phthalic anhydride leading to better combustion of the phthalic anhydride for the acidic and amphoteric metal oxides. For the basic metal oxides, the magnesium oxide addition would decrease the combustion of phthalic anhydride. The research also found that the ratio of transition metal oxide per magnesium oxide should be at an appropriate ratio to keep a balance between the adsorption of phthalic anhydride and the catalytic activity of the transition metal oxides. Magnesium oxide promoted the adsorption of phthalic anhydride leading to better combustion of the phthalic anhydride for the acidic and amphoteric metal oxides [Tongsang (2001), Umpon (2001), Nuampituk (2002) and Nugoolchit (2002)].

The idea of this work was to modify the spent catalyst for it could be used in the other reactions instead of discharging the spent catalyst as waste. Therefore, the aim of this research was to study the possibility to improve the spent phthalic anhydride catalyst for being used as a catalyst in the combustion of phthalic anhydride

by prepared the V_2O_5 /TiO_2 catalyst which the same composition as the industrial catalyst for the production of phthalic anhydride. Then the catalysts promoted with transition metals and magnesium oxide were tested as catalysts for the combustion of phthalic anhydride.

In this study the V-Mg-O/ TiO_2 catalyst with different transition metals (Fe, Cu, Zn and Mo) had been used to investigate the oxidation properties of these catalysts for phthalic anhydride reactants.

This present work is organized as follows:

Chapter II contains literature reviews of phthalic anhydride process, transition metal oxide and supported transition metal oxide catalysts on various reactions.

The theory of this research, studies about the oxidation reaction and its possible mechanisms, the reaction of anhydrides, and the properties of transition metal oxides are presented in chapter III.

Description of experimental systems and the operational procedures are described in chapter IV.

Chapter V reveals the experimental results of the characterization of Fe-V-Mg-O/ TiO_2 , Cu-V-Mg-O/ TiO_2 , Zn-V-Mg-O/ TiO_2 and Mo-V-Mg-O/ TiO_2 catalysts and the oxidation reaction of phthalic anhydride over these catalysts.

Chapter VI contains the overall conclusion emerged from this research.

Finally, the sample of calculation of catalyst preparation, external and internal diffusion limitations, calibration curves from area to mole of phthalic anhydride, and carbon dioxide, and data of the experiments which had emerged from this study are included in appendices at the end of this thesis.

CHAPTER II

LITERATURE REVIEW

The heterogeneous catalytic oxidation on transition metal oxides was extensively used in catalysis for selective and total oxidation processes. The complete catalytic oxidation was a widely used method for elimination of organic pollutants in gaseous streams to CO₂ and water. A large body of literature was concerned with the development of catalysts for this reaction. For many researches, transition metal oxide catalysts can completely oxidise organic compounds.

This chapter reviews the works about the combustion of phthalic anhydride on Cr, Mn, Fe, Co, Ni, Cu, Zn, Mo and W promoted MgO on Al₂O₃ supported catalysts and V-Mg-O/TiO₂, the processes for recovery of phthalic anhydride, the treatment of byproducts obtained in the preparation of phthalic anhydride, the deactivation of an industrial V₂O₅/TiO₂ catalyst for oxidation of o-xylene into phthalic anhydride, the transition metal oxide and supported transition metal oxide catalysts in the various reactions.

2.1 Literature reviews

Toyada and Teraji (1980) invented a process that allows the treatment of byproducts obtained in the preparation of phthalic anhydride without creating secondary pollution. Byproducts were treated by heating the byproducts to a temperature sufficient to maintain the byproducts in a molten state and thereafter atomizing air having a temperature of at 60°C for combustion. The byproducts may be low boiling point and/or high boiling point fractions obtained in the purification step by distillation of crude phthalic anhydride produced by the partial oxidation of ortho-xylene or naphthalene.

Keuneche *et al.* (1981) invented a process for continuously separating phthalic anhydride from the reaction gases of the catalytic oxidation of o-xylene and/or naphthalene by treating reaction gas mixture with a maleic anhydride absorbent.

Even though pure maleic anhydride could be used as an absorbent, maleic anhydride containing phthalic anhydride was usually used so as to keep the costs of regenerating the absorbent within economical bounds. Thus, maleic anhydride could contain up to 85% by weight phthalic anhydride. Absorption could be performed in two or more stages, preferably in two stages. The reaction gas, with a temperature from 135 - 150° C, was introduced into the absorption zone, and withdrawn at a temperature from 45 - 80°C from the absorption zone. The maleic anhydride, which was loaded with phthalic anhydride, was separated through distillation into raw phthalic anhydride as a bottoms product and an overhead product primarily containing maleic anhydride. The overhead product was then returned into the absorption zone. The raw phthalic anhydride was treated and then purified through distillation, e.g. in a continuous, two stage distillation in which light, volatile impurities, such as residual maleic anhydride and benzoic acid, were distilled off in the first stage and the pure phthalic anhydride was distilled in the second as an overhead product. The gas leaving the absorption zone and containing small amounts of maleic anhydride was scrubbed with water. The maleic acid solution recovered from this scrubbing was evaporated, the maleic acid was dehydrated and distilled, and a part of the maleic anhydride distillate was returned into the absorption zone.

Way and Peter (1981) invented an apparatus for recovery of vaporized phthalic anhydride from the gas streams. Phthalic anhydride was recovered from gases in a multiple heat-pipe exchanger system, one or more for condensing phthalic anhydride from gases containing vapors thereof and one or more simultaneously melting out the condensed phthalic anhydride solids. The exchangers being switched in alternate cycles to melt out from the surfaces of the exchanger tube ends on which the phthalic anhydride solids were first accumulated, and to condense phthalic anhydride solids in the exchanger from which the phthalic anhydride was cleared by melting out. The cooling to recover phthalic anhydride was carried out with ambient air, and the heating to melt out accumulated phthalic anhydride was effected with hot gases.

McCabe and Mitchell (1983) studied the oxidation of ethanol and acetaldehyde over alumina supported catalysts. They found that Pt/Al₂O₃ catalysts

were only slightly more active than metal oxide catalysts for the same volume in the combustion of ethanol.

Yao (1984) studied the catalytic oxidation of ethanol at low concentrations. The catalysts used included Pt, Pd, Rh, Ag, and the first row transition metal oxide, all supported on Al_2O_3 or ZrO_2 . Of the base metal oxide catalysts, $\text{CuO}/\text{Al}_2\text{O}_3$ had the highest activity for total oxidation to CO_2 .

Wachs *et al.* (1985) studied the interaction of vanadium pentoxide with titania (anatase) effected on *o*-xylene oxidation to phthalic anhydride. It was found that two types of vanadia were present in active $\text{V}_2\text{O}_5/\text{TiO}_2$ (anatase) catalysts: a surface vanadia species coordinated to the TiO_2 support and crystallites of V_2O_5 . Then suggested that the surface vanadia was the active site in $\text{V}_2\text{O}_5/\text{TiO}_2$ (anatase) catalysts for the oxidation of *o*-xylene to phthalic anhydride. The TiO_2 (anatase) support had to be covered by a complete monolayer of the surface vanadia species since exposed titania sites lead to complete combustion of the partial oxidation products. The crystalline V_2O_5 phase was not as effective for this oxidation reaction. They also reported that moderate amounts of crystalline V_2O_5 did not significantly affect the catalytic performance of $\text{V}_2\text{O}_5/\text{TiO}_2$ (anatase) because of the low effective surface area and poor catalytic activity of this phase. Thus, the TiO_2 (anatase) support modified the properties of vanadia through the formation of a monolayer of surface vanadia species whose properties were related to the vanadia-titania interaction.

Charr *et al.* (1987) reported that the V-Mg-O catalysts were quite selective for the oxidative dehydrogenation of butanes and butadiene. The active and selective component of V-Mg-O catalyst were the compound magnesium orthovanadate, $\text{Mg}_3(\text{VO}_4)_2$. No oxygenated product was formed over V-Mg-O catalyst. They could not observe characteristic $\text{V}=\text{O}$ stretching in the V-Mg-O. Thus they suggested that the vanadium oxide in V-Mg-O did not form a layer structure of V_2O_5 on the MgO surface. They also reported that the selectivity for the oxidative dehydrogenation increased with decreasing oxygen-to-butane ratio, decreasing conversion and decreasing temperature. A selectivity of up to 60% was obtained. The high selectivity for the oxidative dehydrogenation instead of oxygenate production was

attributed to two factors: the basic surface which facilitated desorption of basic butanes and butadiene, and the absence of V=O which lowered the oxidation activity of the surface.

Spivey (1987) reviewed the complete catalytic oxidation of volatile organics. Both metal oxides and supported noble metals were active for many deep oxidations. (The mechanism of deep catalytic oxidation involved both lattice and surface oxygen for metal oxides and probably reduced metal sites for supported noble metals.) Metal oxide catalysts were generally less active than were supported noble metals, but they were somewhat more resistant to poisoning. This poison resistance may be due to the high active surface area of metal oxides compared to supported noble metals. The most active single metal oxide catalysts for complete oxidation for a variety of oxidation reactions were usually found to be oxides of V, Cr, Mn, Fe, Co, Ni and Cu. The mechanism of oxidation on these oxide catalysts was generally thought to involve strong adsorption of the organic compound at an anionic oxygen site in the oxide lattice leading to the formation of an activated complex. This complex could then react further to yield products of complete combustion.

Vassileva *et al.* (1989) studied the relationship between catalytic activity in the complete oxidation of benzene and the structure of supported vanadium oxide catalysts modified by palladium. From the results, they concluded that the introduction of palladium caused a considerable enhancement of the catalytic activity of the supported vanadium oxide at both 250 and 400°C. The promoting effect of palladium was related to the activation of oxygen and the transition of oxygen and the transition of the low valent vanadium species to V⁵⁺.

Bond (1991) reviewed the vanadium oxide monolayer catalyst. The effect of calcination temperature on the 7% V₂O₅/TiO₂ (anatase) catalyst was found that, with increasing calcination temperature, the surface area of the catalyst decreased and TiO₂ (anatase) transformed to TiO₂ (rutile). The paper also reported that the anatase to rutile transformation was accompanied by a decrease in the content of crystalline V₂O₅.

Corma *et al.* (1993) studied a series of V-Mg-O catalysts using MgO or magnesium oxalate and aqueous solutions of vanadyl-oxalate or ammonium metavanadate as vanadium sources. Large differences in the V/Mg surface atomic ratios were observed on the different catalysts after calcinations, indicating differences in the V-Mg interaction, which were related to the catalysts preparation procedure. These differences were explained by the chemical modification that occurred in the vanadium or magnesium starting materials during the impregnation step. In addition, a new preparation procedure of V-Mg-O catalysts which allowed a homogeneous dispersion of vanadium along the catalyst was presented. By X-ray diffraction, IR, UV-VIS and X-ray photoelectron spectroscopic characterization of the samples before and after the calcinations step, different Mg- and V- compounds had been observed. Before the calcinations step, Mg(OH)₂ and/or magnesium-oxalate, as well as V⁵⁺ and/or V⁴⁺ species, depending on vanadium sources and vanadium content, were observed. After the calcinations step, the formation of magnesium vanadates depended only on the vanadium content of the catalysts. Mg₃V₂O₈ was formed at low vanadium content of the catalyst and Mg₃V₂O₈ + α-Mg₂V₂O₇ at high vanadium content. However, the crystallinity of the magnesium vanadate phases, as well as the distribution of vanadium along the support strongly depended on the preparation procedure.

Hess *et al.* (1993) studied catalysts containing metal oxides for use in the degenerative oxidation of organic compounds presented in exhaust gases from combustion plants. A metal oxide containing catalysts which contained oxides of titanium and/or zirconium, oxides of vanadium and/or niobium and oxides of molybdenum, tungsten, and chromium. It was found that the adding of alkaline earth metal sulfates produced a catalyst which was clearly superior to catalysts composed only of the metal oxides. The catalyst they preferred contained the following components: titanium dioxide, especially in the form of anatase, vanadium oxide in the form of V₂O₅ and tungsten oxide in the form of WO₃.

Ramis and Busca (1993) investigated the effect of dopants and additive on the state of surface vanadyl centers of vanadia-titania catalysts. They observed that the V=O stretching frequency and its first overtone on vanadia-titania-based catalysts

were sensitive to the presence of dopants and additives. Alkali and alkali earth metal cations decreased strongly the V=O stretching frequency. Doping of TiO₂ and of vanadia-titania with alkali cations caused the formation of new stronger basic sites. Vanadyl cations, that were Lewis acidic, probably were attracted by these new stronger basic sites and O=V-O-Ti bridges were substituted by O=V-O-M bridges (M= alkali or alkali earth cation). As a result of the increased basicity of ligands, coordinatively unsaturated vanadyl centers have their Lewis acidity weakened.

Weng and Lee (1993) studied the effect of Nb₂O₅ promoter on V₂O₅/TiO₂ catalysts for selective catalytic reduction (SCR) of nitric oxide. It was found that both the active sites and the acid sites increased with the content of Nb₂O₅ due to the increase in BET surface area. The activities of the SCR reaction and the ammonia oxidation were enhanced by the Nb₂O₅ promoter in the lower and higher temperature ranges, respectively.

Kang and Wan (1994) studied the effects of acid or base additives on the catalytic combustion activity of chromium and cobalt oxides. It was found that the base additive could enhance the catalytic activity of Cr, Co oxides for carbon monoxide oxidation, but the acid additive reduced the activity. For ethane combustion, the addition of a base additive to the catalysts could reduce the ethane conversion. The selectivity of carbon dioxide, however, was increased to 100% because the rate of carbon monoxide oxidation was enhanced. On the other hand, the addition of acid additive to the catalyst gave an increase in ethane conversion, but the selectivity to carbon dioxide was reduced.

Grabowski *et al* (1995) studied the effect of alkaline promoters on catalytic activity of V₂O₅/TiO₂ and MoO₃/TiO₂ catalysts in oxidative dehydrogenation of propane and in isopropanol decomposition. For both types of catalysts the total activity in oxidative dehydrogenation of propane decreased in the sequence: V(Mo)/Ti ≥ 1V(Mo)/TiLi > 1V(Mo)/TiK > 1V(Mo)/TiRb. The decrease in the activity may be due to blocking of the propane activation centers, which follow the order of decreasing electronegativity of the alkaline promoters. These changes in acidic-basic properties facilitated desorption of propane, preventing its further oxidation on the

surface to CO_x . The addition of alkaline cations also modified the dispersion of the deposited oxides, decreasing the amount of crystalline V_2O_5 and MoO_3 in the promoted catalysts.

Leklertsunthon (1998) investigated the oxidation property of a series of V-Mg-O/ TiO_2 catalyst in the oxidation reaction of propane, propene, 1-propanol and carbon monoxide. It had been found that the catalytic behavior of the catalyst depended on the reactants. Propene and CO_2 were the major products in the propane oxidation reaction. The vanadium and magnesium contents affected the catalytic property of the V-Mg-O/ TiO_2 catalyst in the reaction. The sequence of magnesium loading also affected the structure and catalytic performance of this catalyst. In addition, this catalyst was inactive for propene oxidation, from which it could be indicated that propene formed in propane oxidation reaction was not further oxidized to CO_2 . According to 1-propanol oxidation, propionaldehyde was the main observable product at low reaction temperatures, and it was oxidized rapidly to CO_2 when the reaction temperature was increased. Moreover, the dehydration of 1-propanol became significant at high temperatures. It was found that the sequence of magnesium loading and magnesium content had no effect on the catalytic performance of the catalyst. On the other hand, increasing vanadium content improved the propene selectivity and decreased the CO_2 selectivity. Finally, in CO oxidation, this catalyst was rather inactive. Since CO was an unobservable product in propane, propene and 1-propanol reactions, on the V-Mg-O/ TiO_2 catalysts, CO was not produced in these three reactions.

Mongkhonsi and Kershenbaum (1998) studied the effect of deactivation of a $\text{V}_2\text{O}_5/\text{TiO}_2$ (anatase) industrial catalyst on reactor behavior during the partial oxidation of o-xylene to phthalic anhydride. From elemental C-H-N analysis, the results for catalyst pellets aged under a variety of operating conditions was found that some carbonaceous materials could deposit on the catalyst surface at most high reaction temperature, especially at high hydrocarbon concentration. The XRD and XPS results did not reveal the presence of vanadium oxides of V valiancy $< 5+$. The presence of carbon on the used catalyst pellet and the absence of any low oxidation state of vanadium from the XRD and XPS analyses indicated that the deposition of some carbonaceous materials was likely to be a major cause of catalyst deactivation

when it was used in regions high hydrocarbon concentration. This deposited carbon compounds may slow down the reaction rate by a fouling process which reduced the effective activity surface area of the catalyst for further hydrocarbon adsorption. To effectively removed all the adsorbed compounds, the catalyst required reaction in an air stream at a temperature not less than 400°C over several hours, depending upon the past history of the catalyst.

Amiridis *et al.* (1999) studied the effect of metal oxide additives on the activity of V_2O_5/TiO_2 catalysts for the selective catalytic reduction of nitric oxide by ammonia. The results showed, the presence of the second metal oxide phase had different effects on the SCR activity of the V_2O_5/TiO_2 catalyst depending on the nature of the additive. MoO_3 , WO_3 and Nb_2O_5 additive promoted the SCR activity, GeO_2 , FeO_3 and CeO_2 had no significant effect on it, and finally MnO_2 , Ge_2O_3 , La_2O_3 , SnO_2 and ZnO appeared to poison it. The results of this effort indicated that the presence of the additive metal oxides may affect a variety of catalyst properties, including the structure and reducibility of vanadia, and the overall amount and type of surface acidity. Among these factors the only one that correlated with SCR reactivity was the amount of surface Brønsted acid sites on the catalyst surface results in an increase in the SCR rate.

Lietti *et al.* (1999) studied the characterization and reactivity of $V_2O_5-MoO_3/TiO_2$ de- NO_x SCR catalysts. The results showed that the $V_2O_5-MoO_3/TiO_2$ catalysts were very active in the reduction of NO by NH_3 , and exhibited a higher reactivity with respect to the corresponding binary V_2O_5/TiO_2 and MoO_3/TiO_2 samples having the same V and Mo loading. The addition of Mo and V caused the formation of Brønsted sites and of stronger Lewis acid sites, if compared to TiO_2 .

Saracco *et al.* (1999) investigated the oxidation property of Mg-doped $LaMnO_3$ perovskite catalysts on the combustion of methane. The results showed that Mg substitution in the basic $LaMnO_3$ perovskite had a positive effect on the catalytic activity only at low x values ($LaMn_{1-x}Mg_xO_3$). The simultaneous synthesis of perovskite and MgO crystals was proved to be an effective mean to reduce the

sintering tendency of the catalyst and thus allowing to keep small-size perovskite crystals and fair catalytic activity at high temperature.

Chaiyasit (2000) investigated the selective oxidation reaction of 1-propanol and 2-propanol over Co-Mg-O/TiO₂ (8wt%Co, 1wt%Mg) catalyst. It was found that the oxidation property of Co-Mg-O/TiO₂ catalyst depended on type of the reactants. Propionaldehyde was the main product for selective oxidation of 1-propanol. In case of 2-propanol oxidation reaction, it was found that Co-Mg-O/TiO₂ catalyst was an active catalyst for selective oxidation reaction. The main product at low reaction temperature was propylene while at high reaction temperature the main reaction products were propylene and propionaldehyde. From the result of propylene oxidation, it could be indicated that propionaldehyde was produced directly from propylene. In addition, the sequence of cobalt and magnesium loading had no effect on the structure and catalytic performance of this catalyst. While the type of support affected the selectivity of supported cobalt catalyst.

Tongsang (2001) studied the oxidation property of the V-Mg-O/TiO₂ catalysts on the combustion of phthalic anhydride and maleic anhydride. From the results, the MgO modified V₂O₅/TiO₂ catalysts could better oxidize the anhydride ring than the unmodified one. Additionally, the appropriate ratio of vanadium per magnesium led to a balance between the adsorption of the anhydrides and the catalytic activity of vanadium and titania support.

Umpon (2001) investigated the oxidation property of the Co-Mg-O/Al₂O₃ catalyst on the combustion of phthalic anhydride and maleic anhydride. The results showed that magnesium promoted the adsorption of anhydride leading to better combustion of the anhydrides. The research also found that the ratio of cobalt per magnesium should be at an appropriate ratio to keep a balance between the adsorption of the anhydrides and the catalytic activity of cobalt and alumina support.

Centeno *et al.* (2002) investigated the catalytic oxidation of n-hexane, benzene and 2-propanol on Au/CeO₂/Al₂O₃ and Au/Al₂O₃ catalysts. It was showed that ceria enhanced the fixation and final dispersion of gold particles, leading to stabilize them in lower crystallite size. Catalytic results showed that ceria improved the activity of

gold particles in the oxidation of the tested volatile organic compounds (VOCs) probably by increasing the mobility of the lattice oxygen and controlling and maintaining the adequate oxidation state of the active gold particles.

Kim (2002) studied the catalytic oxidation of aromatic hydrocarbons over supported metal oxides. The catalytic activity of metals (Cu, Mn, Fe, V, Mo, Co, Ni, Zn)/ γ -Al₂O₃ was investigated to bring about the complete oxidation of benzene, toluene and xylene. Among them, Cu/ γ -Al₂O₃ was found to be the most promising catalyst from the viewpoint of activity. Increasing the calcination temperature resulted in decreasing the specific surface areas of catalysts, subsequently the catalytic activity. The copper loadings on γ -Al₂O₃ had a great effect on catalytic activity, and 5 wt% Cu/ γ -Al₂O₃ catalyst was observed to be the most active. The activity of 5 wt% Cu/ γ -Al₂O₃ with respect to the VOC molecule was observed to follow the sequence: toluene > xylene > benzene, indicating that the combination of the catalyst property and the physicochemical property of the reactant plays an important role in activity.

Nuampituk (2002) investigated the oxidation property of the Cr, Mn, Mo, W, Fe and Zn promoted MgO on Al₂O₃ supported catalysts on the combustion of phthalic anhydride. It was found that the loading sequence of the metal affected the catalytic activity by changing the number of the surface basic sites. The effects would be positive or negative depended on the type of transition metal and the amount of the magnesium selected. If the amount of magnesium selected was lower than the optimum amount, the procedure that resulted in a larger number of the surface basic site would yield a catalyst with higher catalytic activity. On the other hand, if the amount of magnesium selected was higher than the optimum amount, the procedure that resulted in a larger number of the surface basicity would decrease the catalytic activity.

Nugoolchit (2002) investigated the effects of MgO on the oxidation property of the transition metal oxide catalysts on the combustion of phthalic anhydride. The results showed that magnesium oxide promoted the adsorption of phthalic anhydride leading to better combustion of the phthalic anhydride for the acidic and amphoteric metal oxides. For the basic metal oxides, the magnesium oxide addition would

decrease the combustion of phthalic anhydride. The research also found that the ratio of transition metal oxide per magnesium oxide should be at an appropriate ratio to keep a balance between the adsorption of the phthalic anhydride and the catalytic activity of the transition metal oxides.

Paola *et al.* (2002) studied the catalytic photo oxidation reactions with aliphatic and aromatic organic compounds having different acid strengths. The catalysts were TiO₂ powders doped with various transition metal ions (Co, Cr, Cu, Fe, Mo, V and W). The co-doped powder showed to be more photoactive than the bare TiO₂ for methanoic acid degradation while the behavior of TiO₂/Cu and TiO₂/Fe was similar to that of the support. TiO₂/W was the most efficient sample for the photo degradation of benzoic acid and 4-nitrophenol, TiO₂ the most active powder for ethanoic acid.

Anastasov (2003) studied the deactivation of an industrial V₂O₅-TiO₂ catalyst for oxidation of o-xylene into phthalic anhydride. The industrial reactor contained 10550 tubes of 26 mm inner diameter and 3250 mm length. The catalyst was loaded in the tubes, while a molten salt NaNO₂/KNO₃ circulating in the shell-side removed the heat generated by the reactions. The catalyst was a V₂O₅-TiO₂ (anatase) supported catalyst. The weight ratio V₂O₅/TiO₂ was 0.06, the catalyst being promoted by rubidium and phosphorus. The active substance (0.1 mm thick) was laid over porcelain ring in order to increase the contact surface. The sizes of a ring were height 6 mm, outside and inside diameters 8.4 and 4.6 mm, respectively. There were three to four pellets on a tube diameter. The length of the bed was 280 cm, while its bulk density was about 1500 kg/m³. From the results, the very low activity of a catalyst being 60.5 months old in the region after 100 cm of the bed, was most probably due to a reversible deactivation caused by tar products blocking the active site. Therefore, the catalyst must be removed after 5 years use.

2.2 Comment on previous works

From the above reviewed literature, it could be seen that transition metal oxides showed the high activity of oxidation the organic compounds. Furthermore, the result of the combustion of phthalic anhydride on Cr, Mn, Fe, Co, Ni, Cu, Zn, Mo and W promoted MgO on Al₂O₃ supported catalysts and V-Mg-O/TiO₂ showed that MgO could promote the adsorption of phthalic anhydride leading to better phthalic anhydride combustion for the acidic and amphoteric metal oxides. For the basic metal oxides, the magnesium oxide addition would decrease the combustion of phthalic anhydride. The research also found that the ratio of transition metal oxide per magnesium oxide should be at an appropriate ratio to keep a balance between the adsorption of the phthalic anhydride and the catalytic activity of the transition metal oxides. However, there was no information about the effect of transition metal and MgO loading on the V₂O₅/TiO₂ catalyst in the combustion of phthalic anhydride. In this research, the system consisted of transition metal oxide (Fe, Cu, Zn and Mo), MgO and V₂O₅/TiO₂ to study the catalytic property in the combustion of phthalic anhydride.

CHAPTER III

THEORY

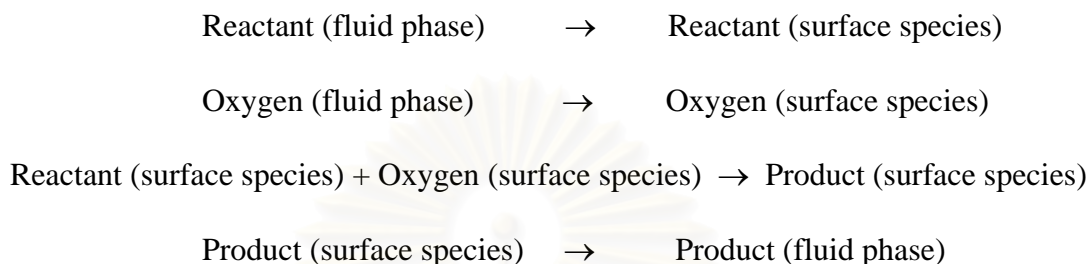
Catalytic oxidation can be categorized as complete oxidation and selective oxidation. Complete oxidation is the combustion of organic compounds to the combustion products; CO_2 and H_2O [Thammanonkul (1996)]. It is a practicable method for the elimination of organic pollutants in gaseous streams. The selective oxidation is the reaction between hydrocarbon and oxygen to produce oxygenates (such as alcohols, aldehydes, carboxylic acids which are produced from partial oxidation processes) or unsaturated hydrocarbons (such as ethane and propene which can be produced from oxidative dehydrogenation process) [Thammanonkul (1996)].

In studies on oxidative catalysis, commonly great attention is attached to the state of oxygen on the catalyst surface. A relative inert oxygen molecule is activated by interacting with the surface of an oxide catalyst. The main parameter determining oxygen reactivity on the catalyst is the energy of oxygen binding with the catalyst as a thermochemical characteristic. Correlation between rates of catalytic oxidation and oxygen binding energy on oxide catalysts have been established. The weaker the oxygen binding with the catalyst surface, the more efficient is complete oxidation with this catalyst [Satterfield (1980)].

With oxide catalysts, chemisorbed surface oxygen as well as lattice oxygen may play a role. The oxidation of propylene to acrolein on a BiMo/SiO_2 catalyst in a pulsed reactor showed that surface chemisorbed oxygen as well as lattice oxygen could contribute to the overall reaction. It seemed plausible that in many other cases chemisorbed oxygen would lead to a different set of products than lattice oxygen and both mechanisms could be significant. On the basis of other studies advanced the hypothesis that surface-adsorbed oxygen may in general lead to products of complete oxidation and the lattice oxygen is needed for partially oxidized products [Satterfield (1991)].

3.1 Mechanism of oxidation reaction

The mechanism of oxidation reaction between a reactant and an adsorbed surface oxygen species on a catalyst surface can be shown as follows:



3.2 Magnesium promoted transition metal oxide catalysts

Transition metal oxides were interesting materials in the field of heterogeneous catalysis. The most active single metal oxide catalysts for complete oxidation for a variety of oxidation reactions were usually found to be oxides of V, Cr, Mn, Fe, Co, Ni, and Cu. For the complete oxidation of methane, methanol, ethanol, acetaldehyde, and ethanol/methanol mixture, the transition metal oxide catalysts exhibited high activity. The $\text{CuMn}_2\text{O}_4/\text{Al}_2\text{O}_3$ catalyst was more active than the $\text{CuO}_x/\text{Al}_2\text{O}_3$ and $\text{Mn}_2\text{O}_3/\text{Al}_2\text{O}_3$ catalyst for the complete oxidation of CO, ethyl acetate, and ethanol. The $\text{MoO}_3/\text{SiO}_2$ was the most active catalysts among the $\text{MoO}_3/\text{support}$ catalysts for the diesel soot oxidation. For the photo-oxidation of benzoic acid, TiO_2/W was the most efficient catalyst.

MgO was white powder that usually obtained by dehydration of magnesium dihydroxide. Its catalytic interest lied in its essentially basic surface character, which made it an effective catalyst support. Magnesium oxide was interesting because it had the ability to stabilize metals in unusual oxidation states and to avoid sintering and evaporation of the metal atoms [Aramendia *et al.* (1999)].

3.3 Acidic and Basic Catalyst [Kirk-Othmer (1979)]

The correlation of catalytic efficiency with the strength of the acid or base was of considerable importance. The general theory of acid-base catalysis in which a proton is transferred from the catalyst to the reactant (acid catalysis) or from the reactant to the catalyst (base catalysis). The velocity of the catalyzed change is thought to be determined by a protolytic reaction between the reactant and the catalyst. The molecule, on receiving or giving a proton, is converted into an unstable state which immediately (or very rapidly, compared with the velocity of the protolytic reaction) leads to the reaction under consideration. Thus, acid catalysis of a basic reactant is represented by the general scheme $R+AH^+ \rightarrow RH^++A$, whereas $RH^++B \rightarrow R+BH^+$ represents basic catalysis of an acidic reactant.

3.4 Chemisorption at oxide surface [Bond (1987)]

On the basis of their electrical conductivities, solids are traditionally divided into four classes as shown in Table 3.1.

Table 3.1 Classification of solids by electrical conductivity

Class	Conductivity range ($\Omega \text{ cm}^{-1}$)	Chemical class	Examples
Superconductors	up to 10^{35}	metals at low temperatures	-
Conductors	10^4 - 10^6	metals and alloy	Na, Ni, Cu, Pt etc.
Semiconductors	10^3 - 10^8	(a) intrinsic: semi-metals (b) extrinsic: oxides and sulphides of transition and post-transition elements	Ge, Si, Ga, As etc. ZnO, Cu ₂ O, NiO, ZnS, MoS ₂ , NiS etc.
Insulators	10^{-9} - 10^{-20}	Stoichiometric oxides	MgO, SiO ₂ , Al ₂ O ₃ etc.

Of greater interest are the oxides and sulphides whose conduction is due to their departure from precise stoichiometry: these substances are termed *extrinsic* or defect semiconductors. The more non-stoichiometric they are, the greater their conductivity. Another important general feature of semiconductors is that their conductivity increases with temperature according to a relation similar to the Arrhenius equation.

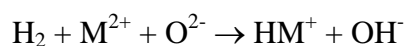
A useful generalization concerning the requirement for p-type semi-conductivity is that the cation shall have an accessible higher oxidation state: thus cobalt(II)oxide and copper(I)oxide are also in this group. For n-type semiconductivity an accessible lower oxidation state (which may include the zero-valent state) is needed: thus cadmium oxide and iron(III)oxide fall in this group (see Table 3.2).

Table 3.2 Classification of semiconducting metal oxides

Effect of heating in air	Classification	Examples
Oxygen lost	Negative (n-type)	ZnO, Fe ₂ O ₃ , TiO ₂ , CdO, V ₂ O ₅ , CrO ₃ , CuO
Oxygen gained	Positive (p-type)	NiO, CoO, Cu ₂ O, SnO, PbO, Cr ₂ O ₃

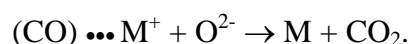
3.4.1 Chemisorption on semiconducting oxides

A qualitative understanding of the chemisorption of simple gases on semiconducting oxides follows simply from their chemistry. Reducing gases such as hydrogen and carbon monoxide are adsorbed strongly, but irreversibly: on heating, only water and carbondioxide respectively can be recovered. Hydrogen probably dissociates heterolytically on adsorption, viz.



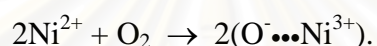
The hydroxyl ion will decompose on heating to form water and anion vacancies, and an equal number of cations will be reduced to atoms.

Carbon monoxide usually chemisorbed first on the cation, whence it reacts with an oxide ion:



Here is the first stage of a process that can lead ultimately to the complete reduction of the oxide to metal. These steps are also similar to those involved in the catalyzed oxidation of these molecules.

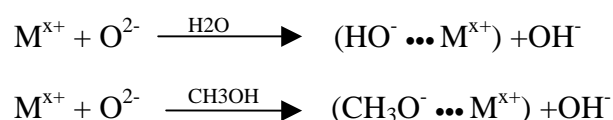
The chemisorption of oxygen on p-type oxides occurs by a mechanism involving the oxidation of Ni^{2+} ions at the surface to Ni^{3+} :



High coverages by the O^- ion can result, and it is easy to see that this is the first step in the incorporation of excess oxygen, referred to above. When the n-type oxides (exemplified by zinc oxide) are exactly stoichiometric, they cannot chemisorb oxygen: when however they are oxygen-deficient, they can chemisorb just as much as is needed to restore their stoichiometry by refilling the anion vacancies and reoxidizing the zinc atoms.

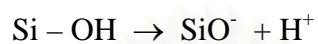
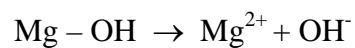
3.4.2 Adsorption on insulator oxides

Since the cations of insulator oxides can be neither oxidized nor reduced, they cannot chemisorb oxygen to any significant extent; they cannot chemisorb hydrogen or carbon monoxide for the same reason. They can, and do, react with water and other polar molecules as:



Indeed under normal circumstances the surface of oxides such as alumina and silica are covered by a layer of chemisorbed water: the surface is then said to be fully

hydroxylated, and indeed these hydroxyl groups are very firmly bound. Their complete removal by heating is almost impossible. When the oxides are suspended in water the M-OH groups can dissociate either as acids or as bases, depending on the electronegativity of the cation, e.g.



The variation of valence electron quantity causes the oxidation number change. These phenomenon leads to the electrical conductivity and acidity change (consider in case of Lewis acid).



สถาบันวิทยบริการ
จุฬาลงกรณ์มหาวิทยาลัย

CHAPTER IV

EXPERIMENTAL

The experimental systems and procedures used in this work are divided into three parts:

1. The preparation of catalysts.
2. The characterization of catalysts.
3. The catalytic activity measurements.

The details of the experiments are described as the following.

The scope of this study

The reaction conditions are chosen as follows:

Catalysts	:	Fe- V-Mg-O/TiO ₂ , Cu- V-Mg-O/ TiO ₂ , Zn-V-Mg-O/ TiO ₂ , Mo- V-Mg-O/ TiO ₂
Reactant	:	C ₈ H ₄ O ₃
Flow rate of reactant	:	100 ml/min
Reaction temperature	:	200-500°C
Space velocity	:	60000 ml g ⁻¹ h ⁻¹

สถาบันวิทยบริการ
จุฬาลงกรณ์มหาวิทยาลัย

4.1 Preparation of catalysts

4.1.1 Chemicals

The details of chemicals used in this experiment are shown in Table 4.1.

Table 4.1 The chemicals used in this experiment.

Chemical	Grade	Supplier
Ammonium molybdate ($(\text{NH}_4)_6\text{Mo}_7\text{O}_{24}\cdot 4\text{H}_2\text{O}$)	Analytical	Univar, Australia
Cupric nitrate trihydrate ($\text{CuN}_2\text{O}_6\cdot 3\text{H}_2\text{O}$)	Analytical	Fluka, Switzerland
Ferric nitrate nonahydrate ($\text{FeN}_3\text{O}_9\cdot 9\text{H}_2\text{O}$)	Analytical	Fluka, Switzerland
Magnesium nitrate ($\text{Mg}(\text{NO}_3)_2$)	Analytical	Fluka, Switzerland
Zinc nitrate hexahydrate ($\text{ZnN}_2\text{O}_6\cdot 6\text{H}_2\text{O}$)	Analytical	Fluka, Switzerland
Titanium oxide (TiO_2)	JRC-TIO1	Department of Material Science, Shimane University
Ammonium metavanadate ($\text{NH}_4(\text{VO}_3)$)	Analytical	Carlo Erba, Italy
Phthalic Anhydride ($\text{C}_8\text{H}_4\text{O}_3$)	Analytical	

4.1.2 Preparation of catalyst

Each catalyst was prepared by 2 steps. The vanadium wet impregnation was the first step in all catalysts. TiO_2 powder was added to an aqueous solution of ammonium metavanadate ($\text{NH}_4(\text{VO}_3)$) at 70°C . The suspension was evaporated at 80°C , then dried in the oven at 110°C in air over night. The resulting solid was calcined in air at 550°C for 6 hours. The second step, the desired metal (Fe, Cu, Zn and, Mo) and magnesium were deposited on the calcined solid by co-impregnation method. The calcined solid was added to an aqueous solution containing both salt of a desired metal and magnesium nitrate $\text{Mg}(\text{NO}_3)_2$ at 70°C , evaporated at 80°C and dried at 110°C in air overnight. After drying the catalyst was calcined in air at 550°C for 6 hours.

4.2 The characterization of catalysts

4.2.1 Determination of composition content of catalysts

The actual composition contents of all the catalysts were determined by atomic absorption spectroscopy (AAS) at the Department of Science Service Ministry of Science Technology and Environment. The calculation of the sample preparation is shown in Appendix A.

4.2.2 BET Surface area measurement

- Apparatus

The apparatus consisted of two gas feed lines for helium and nitrogen. The flow rates of each gas were adjusted by means of fine-metering valves. The sample cell was made from pyrex glass. The BET surface areas were calculated from the amount of the adsorbed N_2 . The amount of the adsorbed N_2 was measured using a gas chromatograph (GC GOW-MAC). The operation conditions of the gas chromatograph (GOW-MAC) is shown in Table 4.2.

Table 4.2 Operation conditions of gas chromatograph (GOW-MAC)

Model	GOW-MAC
Detector	TCD
Helium flow rate	30 ml/min
Detector temperature	80°C
Detector current	80 mA

- Procedure

The mixture of helium and nitrogen gas was flowed through the system at the nitrogen relative gauge pressure of 0.3. The sample was placed in the sample cell, which was then heated up to 150°C and held at this temperature for 2 h. The sample was cooled down to room temperature and ready to measure the surface area. There were three steps to measure the surface area.

(1) Adsorption step

The sample cell was dipped into the liquid nitrogen. Nitrogen was adsorbed on the surface of the sample until equilibrium was reached.

(2) Desorption step

The nitrogen-adsorbed sample was dipped into a water bath at room temperature. The adsorbed nitrogen was desorbed from the surface of the sample. This step was completed when the recorder line return back to the base line.

(3) Calibration step

1 ml of nitrogen gas at atmospheric pressure was injected at the calibration port and the area was measure. The area was the calibration peak.

The BET surface area was calculated using procedures described in Appendix C.

4.2.3 X-ray diffraction (XRD)

The phase structures of the samples were determined by X-ray diffraction, Siemens D 5000 X-ray diffractometer using $\text{CuK}\alpha$ radiation with Ni filter in the 2θ range of 10-80°. The sample was placed into XRD plate before placing on the measured position of XRD diffractometer.

4.2.4 Pyridine Adsorption

The acid site of the samples were determined by the pyridine adsorption. The apparatus consisted of a tube connected to a gas chromatograph (GC9A). The condition of the gas chromatograph is shown in Table 4.3.

Table 4.3 Operation conditions of gas chromatograph (GC9A) for pyridine adsorption

Model	GC9A
Detector	FID
Nitrogen flow rate	30 ml/min
Column temperature	150°C
Detector temperature	180°C
Injector temperature	180°C

0.02 g of catalyst sample was placed in the tube. 0.1 μ l of pyridine was injected to the gas chromatograph and the peak area was measured. The pyridine was injected until the sample was saturated. The acid site of the sample was calculated from the total peak area of the pyridine adsorbed. The pyridine adsorption was calculated using the procedures described in Appendix G.

4.2.5 Maleic anhydride Adsorption

The basic site of the samples were determined by the maleic anhydride adsorption. The apparatus consisted of a tube connected to the gas chromatograph (GC9A). The condition of the gas chromatograph is shown in Table 4.4.

Table 4.4 Operation conditions of gas chromatograph (GC9A) for maleic anhydride adsorption

Model	GC9A
Detector	FID
Nitrogen flow rate	30 ml/min
Column temperature	280°C
Detector temperature	300°C
Injector temperature	300°C

0.03 g of sample was placed in the tube. 0.3 μ l of maleic anhydride aqueous solution of known concentration (0.104 g/ml) was injected to the gas chromatograph and the area was measured. The maleic anhydride was injected until the sample was saturated. The basic site of the sample was calculated from the total peak area of the maleic anhydride adsorbed. The maleic anhydride adsorption was calculated using the procedures described in Appendix G.

4.3 The catalytic activity measurements

4.3.1 Equipment

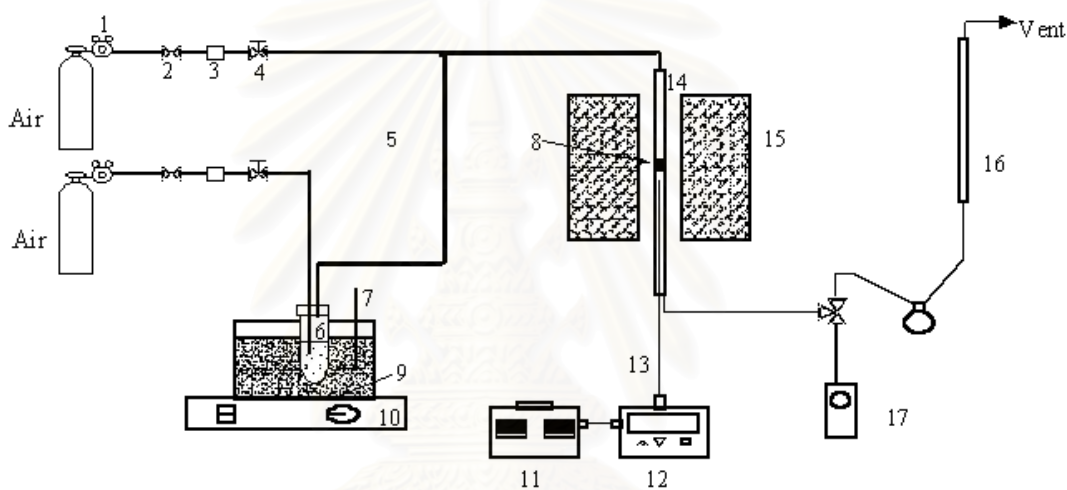
The phthalic anhydride combustion system, as shown in Figure 4.1, consists of a reactor, a saturator, an automatic temperature controller, an electrical furnace and a gas controlling system.

The reactor is made from a stainless steel tube (O.D. 3/8"). Sampling points are provided above and below the catalyst bed. Catalyst is placed between two quartz wool layers.

An automatic temperature controller consists of a magnetic contractor model Telex 87114. Reactor temperature was measured at the bottom of the catalyst bed in the reactor. The temperature control set point is adjustable within the range of 0-800°C at the maximum voltage output of 220 volt.

The electrical furnace supplies heat to the reactor for phthalic anhydride combustion. The reactor can be operated from room temperature up to 800°C at the maximum voltage of 220 volt.

The gas supplying system consists of cylinders of air zero, each equipped with pressure regulators (0-120 psig), on-off valves and fine-meter valves used for adjusting the flow rate.



- | | | |
|-------------------------|----------------------------------|----------------------------|
| 1. Pressure Regulator | 2. On-Off Valve | 3. Gas Filter |
| 4. Metering Valve | 5. Heating Line | 6. Saturator |
| 7. Thermometer | 8. Catalyst Bed | 9. Sand bath |
| 10. Stirring Controller | 11. Variable Voltage Transformer | 12. Temperature Controller |
| 13. Thermocouple | 14. Reactor | 15. Furnace |
| 16. Flow Meter | 17. Sampling Point | |

Figure 4.1 Flow diagram of phthalic anhydride combustion system

The organic composition in the feed and product stream was analyzed by a flame ionization detector gas Chromatograph Shimadzu GC9A.

A Shimadzu GC8A gas chromatograph equipped with a thermal conductivity detector was used to analyze permanent gases and water. Two columns, a 5A molecular sieve to separate oxygen and CO and a Porapak-Q column to separate CO₂ and water were operated in parallel. The operating conditions of the GC are listed in the Table 4.5.

Table 4.5 Operating conditions for gas chromatographs

Gas chromatograph	GC8A	GC9A
Detector	TCD	FID
Column	MS-5A, Porapak-Q	Chromosorb WAW
Carrier gas	He (99.999%)	N ₂ (99.999%)
Carrier gas flow	25 ml/min	30 ml/min
Column temperature	100°C	210°C
Detector temperature	130°C	250°C
Injector temperature	130°C	250°C
Analyzed gas	CO, CO ₂ , H ₂ O	Phthalic anhydride

4.3.2 Oxidation procedure

The oxidation procedures are described in the detail below.

1. 0.1 gram of catalyst was packed in the middle of the stainless steel microreactor located in an electrical furnace.
2. The total flow rate was 100 ml/min. The concentration of phthalic anhydride in air was adjusted to the required values.
3. The reaction temperature was between 200-500°C. The effluent gas was analyzed by using the FID and TCD gas chromatographs. The chromatograph data were changed into mole of phthalic anhydride and CO₂ by calibration curves in Appendix D.

The operating conditions selected have been checked to confirm that there was no external and internal mass transfer resistance. The calculation was shown in Appendix B.



สถาบันวิทยบริการ
จุฬาลงกรณ์มหาวิทยาลัย

CHAPTER V

RESULTS AND DISCUSSION

The results and discussion in this chapter are divided into two major parts including the catalyst characterization and the catalytic combustion reaction of phthalic anhydride, and surface acidity and basicity, respectively.

5.1 Catalyst characterization

5.1.1 Determination of catalyst compositions and BET surface area

The results of metal composition and BET surface area of all catalysts, which are analyzed by Atomic Absorption Spectroscopy (AAS) and N₂ adsorption are summarized in Table 5.1. The weight % of V is 7.1 (as V₂O₅)

Table 5.1 The composition of different metal loading catalysts and BET surface areas

Catalyst	wt% metal	wt% Mg	BET surface area (m ² /g)
TiO ₂	-	-	50.64
V ₂ O ₅ /TiO ₂	-	-	8.83
8Cu- 7V-1Mg-O/TiO ₂	7.9	1.0	7.88
8Fe- 7V-1Mg-O/TiO ₂	7.7	1.1	12.22
8Mo- 7V-1Mg-O/TiO ₂	6.3	0.9	8.99
8Zn- 7V-1Mg-O/TiO ₂	6.8	1.0	7.12

It must be noted here that the amounts of the transition metals and magnesium used in this work have not been proved to be the amounts that yielded the best performance catalyst for each transition metal. The previous works [Nuampituk

(2002), Nugoolchit (2002)] have showed that adding about 1wt% Mg could significantly increase the combustion activity of the catalysts. Mg loading higher than 1wt% may increase or decrease the combustion activity. In case of activity gain, the increase of Mg loading from 1wt% to 4wt% did not strongly increase of the combustion activity as the increase from 0wt% to 1wt%. Therefore, 1wt% Mg was chosen in this work. The amount of the transition metals was fixed at 8 wt% to make the obtained results comparable to the previous works [Nuampituk (2002), Nugoolchit (2002)].

The data in Table 5.1 show that the surface areas of V_2O_5/TiO_2 , 8Cu-7V-1Mg-O/ TiO_2 , 8Fe-7V-1Mg-O/ TiO_2 , 8Zn-7V-1Mg-O/ TiO_2 and 8Mo-7V-1Mg-O/ TiO_2 catalysts were relatively low. However, the surface areas of 8Cu-7V-1Mg-O/ TiO_2 and 8Zn-7V-1Mg-O/ TiO_2 catalyst slightly decreased with addition of transition metal and MgO into V_2O_5/TiO_2 catalyst. For 8Fe-7V-1Mg-O/ TiO_2 and 8Mo-7V-1Mg-O/ TiO_2 catalysts, when the introduction of transition metal and MgO into V_2O_5/TiO_2 catalyst, their surface areas increased.

5.1.2 X-ray Diffraction (XRD)

The first three strongest XRD peaks of transition metal oxides from the reference [The JCPDS (1980)]using $CuK\alpha$ radiation are listed in Table 5.2.

Table 5.2 The reference XRD patterns for transition metal oxides

Oxides	Position (2θ)	Oxides	Position (2θ)
CuO	35.4°, 35.6°, 38.8°	MoO ₃	9.6°, 25.8°, 29.4°
Cu ₂ O	37°, 40.4°, 42.4°	MoO ₂	26°, 36.8°, 53.4°
Fe ₂ O ₃	29.8°, 32.8°, 67.5°	ZnO	33.6°, 58.4°, 62.6°
FeO	61°, 61.4°, 73°	ZnO ₂	31.8°, 37°, 63°
MgO	37°, 43°, 62.8°		

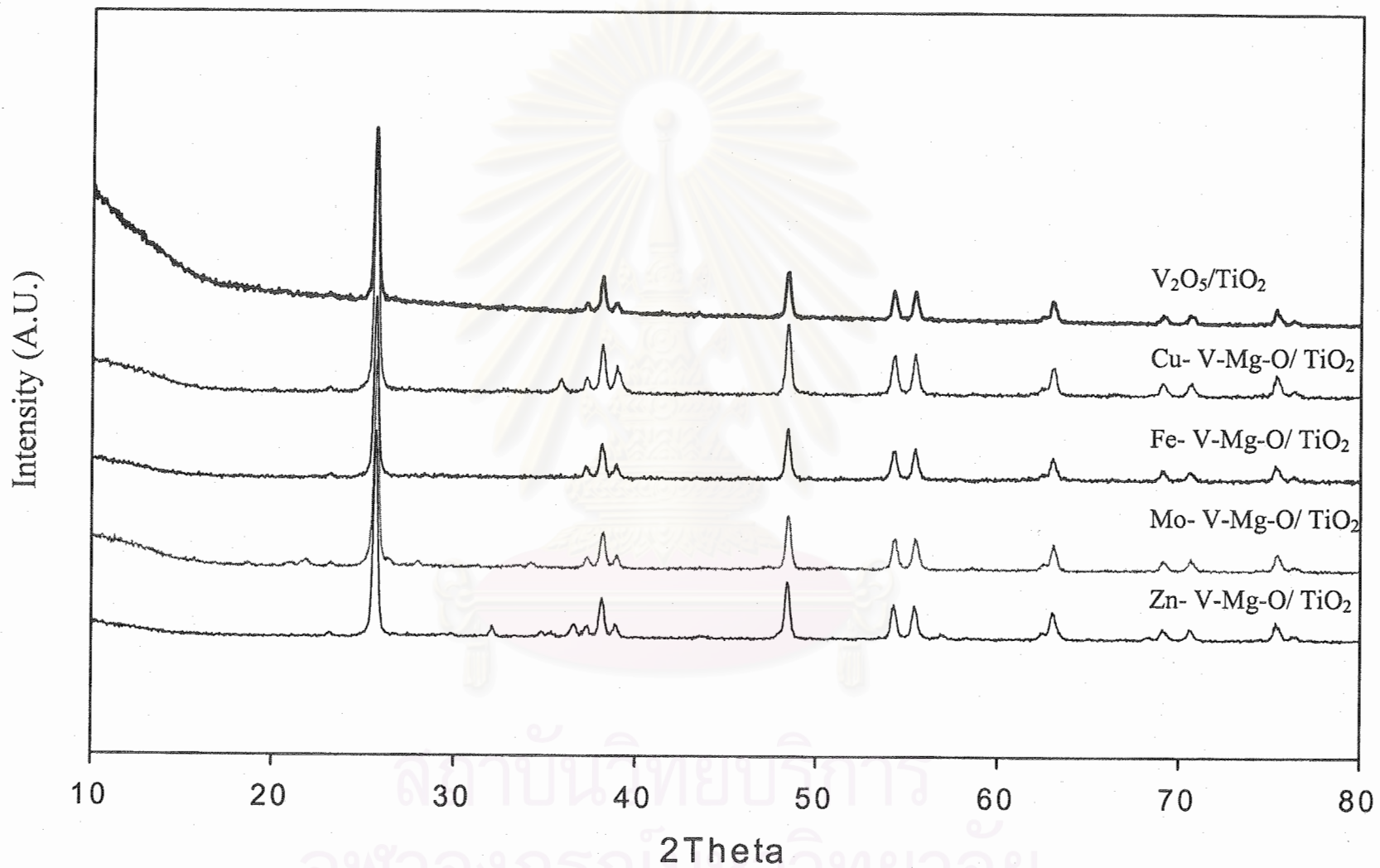


Figure 5.1 The XRD pattern of all catalysts

XRD was used to determine the bulk crystalline phases in the catalysts. The diffraction patterns of all catalysts are shown in Fig 5.1. The XRD pattern of TiO_2 showed strong diffraction peaks at 25.3° , 37.8° , 48.0° , 53.9° and 55.1° indicating the TiO_2 is in the anatase form.

From the XRD result of $\text{V}_2\text{O}_5/\text{TiO}_2$, it was observed that only peaks of TiO_2 were present in the XRD pattern. The peak of vanadium oxide was not detected possibly because the XRD pattern of vanadium oxide was hidden by the XRD pattern of TiO_2 support, or vanadium oxide did not form a crystal with significant size or did not form a crystal. It was also found that the TiO_2 (anatase) support did not undergo structural changes during the vanadia impregnation and calcinations (550°C -6 hr) in the first step because the XRD analysis only exhibited the anatase phase (rutile was not present in the XRD pattern).

After addition of Fe, Cu, Zn and Mo in the second step, different results were observed. The XRD result of $\text{Cu-V-MgO}/\text{TiO}_2$ showed two small diffraction peaks at 35.8° and 38.6° which are belong to CuO .

For $\text{Zn-V-MgO}/\text{TiO}_2$, the introduction of zinc oxide induced the appearance of small peaks of ZnO . These peaks were very weak at 31.9° and 36.4° . The relative intensity of those peaks was much lower compared to the TiO_2 peaks. This observation suggested that CuO and ZnO could form crystal with significant size on the catalyst surface.

Similar diffraction patterns were obtained for $\text{Fe-V-MgO}/\text{TiO}_2$ and $\text{Mo-V-MgO}/\text{TiO}_2$. The XRD results of Fe and Mo showed only the TiO_2 peaks and did not show any peak of these transition metal oxides. The peaks of Fe and Mo oxides were not detected possibly because the XRD patterns of these transition metal oxides were hidden by the XRD pattern of TiO_2 support, the oxides did not form a crystal with significant size or it did not form a crystal.

5.2 Catalytic reaction

Phthalic anhydride comprises of an anhydride functional group and a benzene ring. It was a product in the oxidation of o-xylene. In this work, the effects of MgO on the combustion of phthalic anhydride were received much attention. This reaction was studied in an excess oxygen atmosphere. The combustion reaction was as follows:



There were the studies about the combustion reaction of phthalic anhydride on Cr, Mn, Fe, Co, Ni, Cu, Zn, Mo and W promoted MgO on Al₂O₃ supported catalysts and V-Mg-O/TiO₂. The results showed that MgO could promote the adsorption of phthalic anhydride leading to better phthalic anhydride combustion for the acidic and amphoteric metal oxides. For the basic metal oxides, the magnesium oxide addition would decrease the combustion of phthalic anhydride. The research also found that the ratio of transition metal oxide per magnesium oxide should be at an appropriate ratio to keep a balance between the adsorption of the phthalic anhydride and the catalytic activity of the transition metal oxides. Using data from the previous researchs [Nuampituk (2002), Nugoolchit (2002)], Fe, Cu, Zn and Mo were selected due to their capability to oxidize phthalic anhydride.

- Copper oxide catalyst

Figure 5.2 illustrates the catalytic activity of Cu-V-Mg-O/TiO₂ compared with V₂O₅/TiO₂ for the phthalic anhydride combustion. For Cu-V-Mg-O/TiO₂ catalyst, the conversion of phthalic anhydride rapidly increased from 3 to 76% at temperature range of 200 to 300°C and steadily increased to 95% at 500°C. On the other hand, V₂O₅/TiO₂, phthalic anhydride conversion slightly increased from 1 to 15% at temperature range of 200 to 300°C. After that it raised from 15 to 90% at temperature range of 300 to 450°C and it slightly increased to 91% at 500°C.

Cu-V-Mg-O/TiO₂ catalyst showed the phthalic anhydride conversion higher than V₂O₅/TiO₂ catalyst at temperature range of 200 to 450°C, indicating that copper and magnesium oxide were able to improve the catalytic activity of V₂O₅/TiO₂ catalyst.

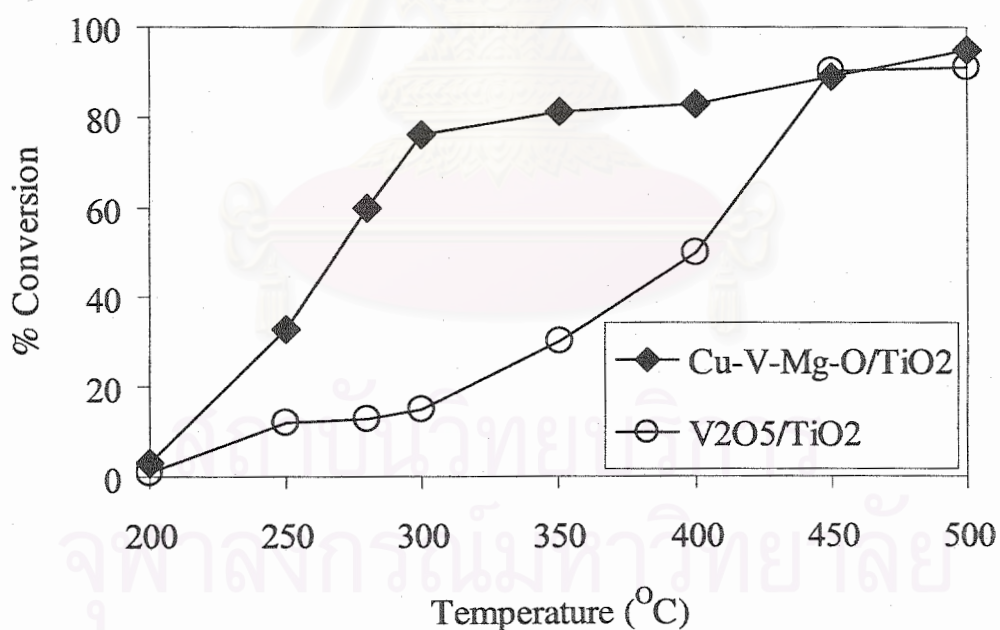


Figure 5.2 The catalytic activity of copper oxide catalysts for the combustion of phthalic anhydride.

- Iron oxide catalyst

Figure 5.3 shows the catalytic activity of Fe-V-Mg-O/TiO₂ compared with V₂O₅/TiO₂ for the combustion of phthalic anhydride. It was found that Fe-V-Mg-O/TiO₂ catalyst exhibited the phthalic anhydride conversion as about 2.7 to 55% in the range of temperature 200 to 300°C and steadily increased until the temperature reached 500°C, which the conversion was about 93%.

Fe-V-Mg-O/TiO₂ catalyst showed the phthalic anhydride conversion higher than V₂O₅/TiO₂ catalyst at temperature between 250 and 450°C, indicating that iron and magnesium oxide were able to catalyze this reaction.

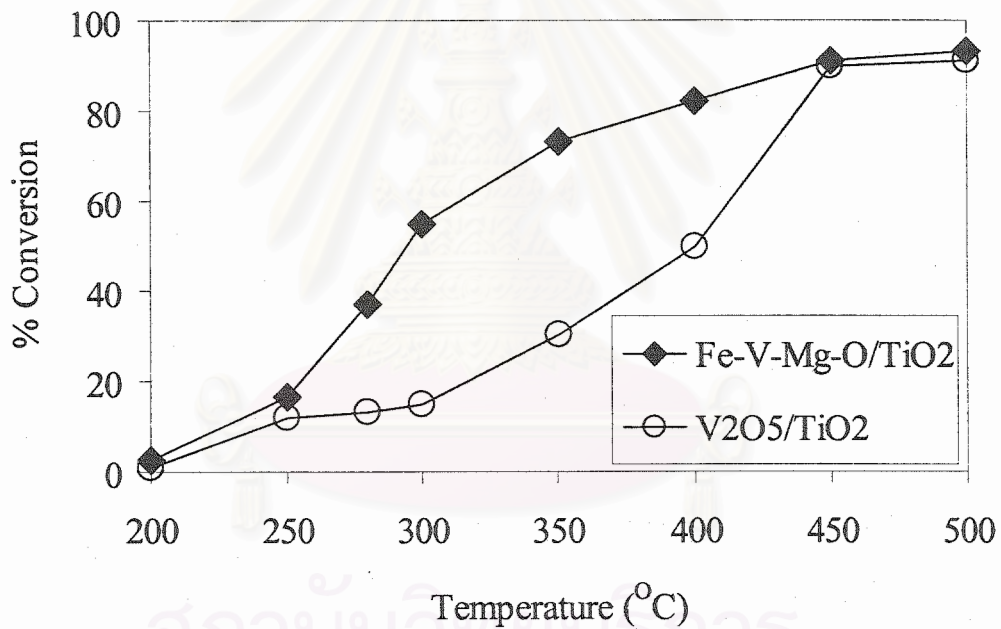


Figure 5.3 The catalytic activity of Iron oxide catalysts for the combustion of phthalic anhydride.

- Zinc oxide catalyst

Figure 5.4 shows the catalytic activity of Zn-V-Mg-O/TiO₂ compared with V₂O₅/TiO₂ for the combustion of phthalic anhydride. It was found that the conversion of phthalic anhydride on Zn-V-Mg-O/TiO₂ catalyst rapidly increased from 5 to 69% at the temperature range of 200 to 300°C. After that it steadily increased until the temperature reached 500°C, which the conversion was about 91%.

The result revealed that loading zinc and magnesium oxide into V₂O₅/TiO₂ catalyst to form Zn-V-Mg-O/TiO₂ catalyst could increase the phthalic anhydride conversion. Especially at the temperature range of 250 to 400°C, it exhibited the phthalic anhydride conversion much higher than V₂O₅/TiO₂, indicating that zinc and magnesium oxide were able to improve the catalytic activity of Zn-V-Mg-O/TiO₂ catalyst.

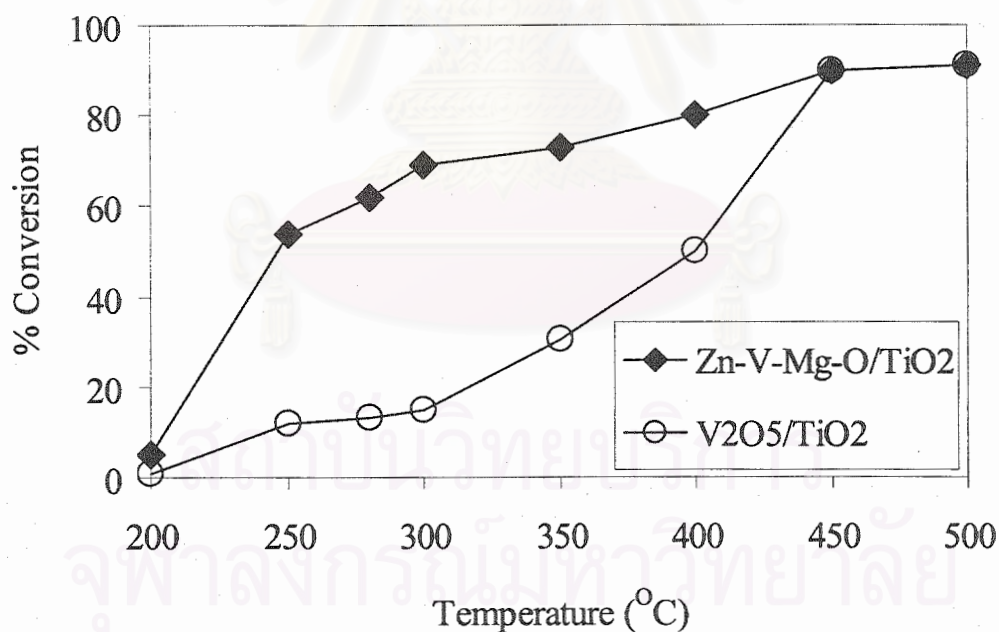


Figure 5.4 The catalytic activity of Zinc oxide catalysts for the combustion of phthalic anhydride.

- Molybdenum oxide catalyst

Figure 5.5 shows the catalytic activity of Mo-V-Mg-O/TiO₂ compared with V₂O₅/TiO₂ for the combustion of phthalic anhydride. It was found that the conversion of phthalic anhydride steadily increased from 8 to 93.5% at temperature range of 200 to 500°C for Mo-V-Mg-O/TiO₂ catalyst.

The result revealed that loading molybdenum and magnesium oxide into V₂O₅/TiO₂ catalyst to form Mo-V-Mg-O/TiO₂ catalyst gave a conversion increase about 25% at temperature range of 280 to 400°C.

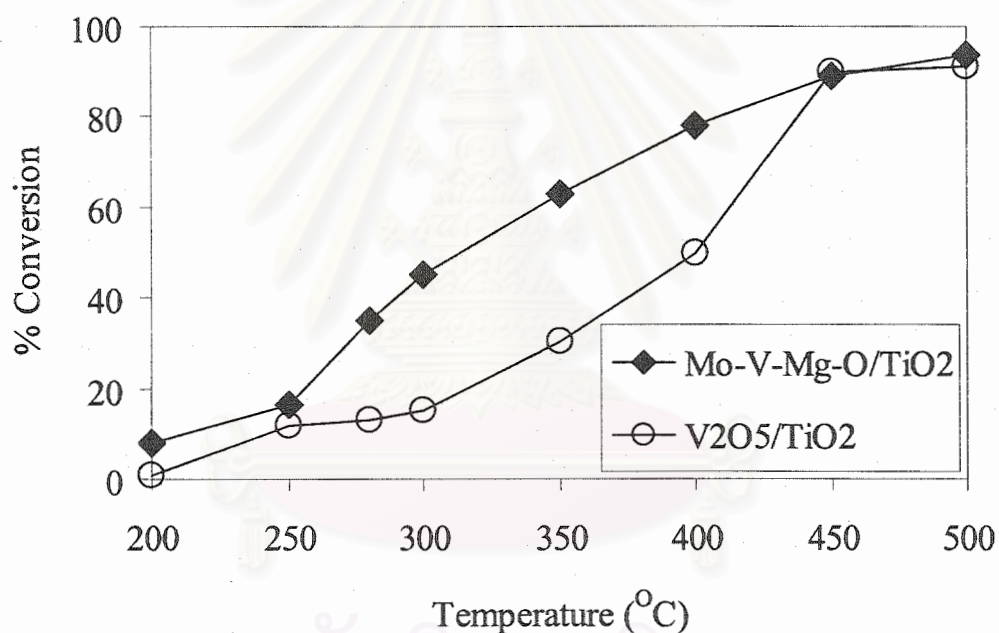


Figure 5.5 The catalytic activity of Molybdenum oxide catalysts for the combustion of phthalic anhydride.

5.3 Activity and surface acidity/basicity

From the results of BET surface area and the XRD result of all catalysts, it was found that there were no simple correlation between the results of catalyst characterization and the catalysts activity observed. Therefore, it was likely that the catalysts activity depended on the amount of acid-basic sites.

The surface acidity and basicity of the catalysts can be quantitatively measured by the amount of pyridine and maleic anhydride adsorption, respectively. The large amount of pyridine adsorption implies the large numbers of acid sites. The large amount of maleic anhydride adsorption implies the large numbers of basic sites. The maleic anhydride also indicated the ability of adsorption of the acidic reactant, phthalic anhydride. Thus, the large amount of maleic anhydride adsorption would have the large numbers of adsorption sites.

From the hypothesis in the previous works [Tongsang(2001), Umpo(2001), Nugoolchit (2002)], the acid site was the active site. The basic site (MgO) would help the adsorption of the acidic reactant, but in the same time, these basic sites would neutralize the acid site (active site). Thus, the maximum activity of the phthalic anhydride combustion needed the optimum between the adsorption of the phthalic anhydride and the catalytic activity of the transition metal oxides.

- Pyridine and maleic anhydride adsorption

The amount of pyridine and maleic anhydride adsorption related to the TiO_2 and the amounts of absorbed pyridine and maleic anhydride of acidic metal oxides are shown in Table 5.1.

Table 5.3 The relative amounts of pyridine and maleic anhydride adsorption and the amounts of absorbed pyridine and maleic anhydride of all catalysts

Catalyst	Pyridine adsorption		Maleic anhydride adsorption	
	Relative	($\mu\text{mole}/\text{m}^2$)	Relative	($\mu\text{mole}/\text{m}^2$)
TiO_2	1.00	0.825	1.00	0.65
$\text{V}_2\text{O}_5/\text{TiO}_2$	2.05	1.690	4.88	3.17
$\text{Cu-V-Mg-O}/\text{TiO}_2$	0.95	0.783	9.18	5.97
$\text{Fe-V-Mg-O}/\text{TiO}_2$	1.09	0.897	5.42	3.53
$\text{Zn-V-Mg-O}/\text{TiO}_2$	1.26	1.039	5.23	3.40
$\text{Mo-V-Mg-O}/\text{TiO}_2$	1.94	1.601	5.10	3.31

The research found that $\text{V}_2\text{O}_5/\text{TiO}_2$ catalyst was not so active for the combustion of phthalic anhydride, possibly because $\text{V}_2\text{O}_5/\text{TiO}_2$ catalyst had the small numbers of the adsorption sites (basic sites) and $\text{V}_2\text{O}_5/\text{TiO}_2$ catalyst did not have the active site or it had the small numbers of the active sites for the combustion of phthalic anhydride. Although titania sites were active for phthalic anhydride combustion, when vanadium oxide was added into the TiO_2 support, the TiO_2 support must be covered by a complete monolayer of the surface vanadia species (>2% $\text{V}_2\text{O}_5/\text{TiO}_2$) with the strong interaction between vanadia and the TiO_2 surface. The surface vanadia species were active for the oxidation of o-xylene to phthalic anhydride than the combustion of phthalic anhydride [Wachs *et al* (1985)].

After loading both transition metal oxide and magnesium oxide into V_2O_5/TiO_2 catalyst, it was found that metal-V-Mg-O/ TiO_2 catalysts give the phthalic anhydride combustion higher than V_2O_5/TiO_2 catalyst, indicating that the transition metals were able to catalyze the reaction. Because the addition of the transition metal oxides to V_2O_5/TiO_2 catalyst would increase the active sites on the surface of catalyst. Moreover, the increment of the maleic anhydride adsorption indicated that the addition of magnesium oxide would increase the numbers of the basic sites on surface of V_2O_5/TiO_2 catalyst and increased the adsorption of phthalic anhydride, thus, provided more opportunity to react with metal, resulting in higher activity.

When considered the effect of types of transition metal oxide on the catalyst activity for the combustion of phthalic anhydride, it was found that Mo-V-Mg-O/ TiO_2 catalyst showed the lowest phthalic anhydride conversion, possibly because Mo-V-Mg-O/ TiO_2 catalyst had lower amount of the adsorption sites (basic sites) compared to other catalyst.



สถาบันวิทยบริการ
จุฬาลงกรณ์มหาวิทยาลัย

CHAPTER VI

CONCLUSIONS AND RECOMMENDATIONS

6.1 Conclusions

The conclusions of the present research are the following:

The addition of transition metal oxides (oxides of iron, copper, zinc and molybdenum) and MgO into the 7V/TiO₂ catalyst to form Fe-V-Mg-O/TiO₂, Cu-V-Mg-O/TiO₂, Zn-V-Mg-O/TiO₂ and Mo-V-Mg-O/TiO₂ catalysts would increase the %conversion of phthalic anhydride combustion.

6.2 Recommendations for future studies

From the previous conclusions, the following recommendations for future studies can be proposed.

1. Transition metal oxide catalysts were suitable to be used in the catalytic combustion of phthalic anhydride. Therefore, it is interesting to further study the oxidation property of these catalysts with other anhydrides. Such as maleic anhydride which is another organic component exists in some industrial effluent gas.

2. It is interesting to study the other metal oxides, which were added into V₂O₅/TiO₂ catalyst to find the best catalyst for anhydride combustion.

3. Further study on the effect of amount of metal and magnesium loading on the oxidation properties of metal-V-Mg-O/TiO₂ catalysts to find an appropriate ratio to provide the highest conversion for phthalic anhydride combustion.

REFERENCES

- Amiridis, M.D., Duevel, R.V., and Wachs, I.E., "The effect of metal oxide additives on the activity of V_2O_5/TiO_2 catalysts for the selective catalytic reduction of nitric oxide by ammonia", *Appl. Catal. B*, 1999, **20**, 111-122.
- Anastasov, A.I., "Deactivation of an industrial $V_2O_5-TiO_2$ catalyst for oxidation of o-xylene into phthalic anhydride", *Chemical Engineering and Processing*, 2003, **42**, 449-460.
- Anderson, J.R., and Pratt, K.C., *Introduction to characterization and testing of catalyst*, Sydney, Academic Press, 1985.
- Aramendia, M. A., Benitez, J. A., Borau, V., Jimenez, C., Marinas, J. M., Ruiz, J. R. and Urbano, F., "Study of MgO and Pt/MgO systems by XRD, TPR, and H MAS NMR", *Langmuir*, 1999, **15**, 1192-1197.
- Bond, G. C., *Heterogeneous Catalysis principles and applications: Chemisorption at oxide surfaces*, Oxford: Clarendon Press, 1987.
- Bond, G.C., "Vanadium oxide monolayer catalysts", *Appl. Catal.* , 1991, **71**, 1-31.
- Centeno, M.A., Paulis, M., Montes, M., and Odriozola, J.A., "Catalytic combustion of volatile organic compounds on Au/CeO₂/Al₂O₃ and Au/Al₂O₃ catalysts", *Appl. Catal. A*, 2002, **234**, 65-78.
- Chaiyasit, N., "Application of the Co-Mg-O/TiO₂ catalyst on the selective oxidation of alcohols", *Master's Thesis, Faculty of Engineering, Chulalongkorn University*, 2000.
- Charr, M.A., Patel, D., Kung, M.C., and Kung, H.H., "Selective oxidative dehydrogenation of propane over V-Mg-O catalysts", *Journal of Catalysis*, 1987, **105**, 483.
- Corma, A., Nieto, J.M.L., and Paredes, N., "Preparation of V-Mg-O catalysts: Nature of active species precursors", *Appl. Catal. A*, 1993, **104**, 161-174.
- Grabowski, R., Grzybowska, B., Samson, K., Sloczynski, J., Stoch, J., and Wcislo, K., "Effect of alkaline promoters on catalytic activity of V_2O_5/TiO_2 and MoO_3/TiO_2 catalysts in oxidative dehydrogenation of propane and in isopropanol decomposition", *Appl. Catal. A*, 1995, **125**, 129-144.
- Hess, K.; Morsbach, B.; Drews, R.; Buechele, W.; and Schachner, H., "Catalyst containing metal oxides for use in the degenerative oxidation of organic

- compounds present in exhaust gases from combustion plants" *United States Patent*, 1993, **5227356**, 1-20.
- Kang, Y.M., and Wan, B.Z., "Effects of acid or base additives on the catalytic combustion activity of chromium and cobalt oxide" *Appl. Catal. A*, 1994, **114**, 35-49.
- Keuneche, G., Klopfer, A., and Sterck, L., "Process for continuously separating phthalic anhydride from the reaction gases of the catalytic oxidation of o-xylene and/or naphthalene", *United States Patent*, 1981, **4285871**, 1-22.
- Kim, S.C., "The catalytic oxidation of aromatic hydrocarbons over supported metal oxide", *Journal of Hazardous Materials*, 2002, **B91**, 285-299.
- Kirk-Othmer. *Encyclopedia of chemical technology: Acidic and Basic catalysts*, John Wiley & Sons, 1979.
- Leklertsunthorn, R., "Oxidation property of the V-Mg-O/TiO₂ catalyst", *Master's Thesis, Department of Engineering, Graduate School, Chulalongkorn University*, 1998.
- Lietti, L., Nova, I., Ramis, G., Dall'Acqua, L., Busca, G., Giamello, E., Forzatti, P., and Bregani, F., "Characterization and reactivity of V₂O₅-MoO₃/TiO₂ De-NO_x SCR catalysts" *Journal of Catalysis*, 1999, **187**, 419-435.
- McCabe, R.W., and Mitchell, P.J., "Oxidation of Ethanol and Acetaldehyde over Alumina-Supported Catalysts", *Ind. Eng. Chem. Prod. Res. Dev.*, 1983, **22**, 212-217.
- Mongkhonsi, T., and Kershenbaum, L., "The effect of deactivation of a V₂O₅/TiO₂ (anatase) industrial catalyst on reactor behaviour during the partial oxidation of o-xylene to phthalic anhydride", *Appl. Catal. A*, 1998, **170**, 33-48.
- Nuampituk, S., "Effect of transition metal and magnesium loading sequence on the combustion of phthalic anhydride over MgO promoted transition metal oxide catalysts" *Master's Thesis, Faculty of Engineering, Chulalongkorn University*, 2002.
- Nugoolchit, J., "Effect of MgO on the combustion of phthalic anhydride over transition metal oxide catalysts" *Master's Thesis, Faculty of Engineering, Chulalongkorn University*, 2002.
- Paola, A.D., Lopez, F.G., Ikeda, S., Marci, G., Ohtani, B., and Palmisano, L., "Photocatalytic degradation of organic compounds in aqueous systems by

- transition metal doped polycrystalline TiO_2 ", *Catalysis Today*, 2002, **75**, 87-93.
- Perry, R.H., and Chilton, C.H., *Chemical Engineering Handbook*, 1973.
- Ramis, G., and Busca, G., "On the effect of dopants and additives on the state of surface of vanadyl centers of vanadia-titania catalysts", *Catal. Lett.*, 1993, **18**, 299-303.
- Reid, R.C., Pranusnitz, J.M., and Poling, B.E., *The Properties of Gases and Liquids*, (n.p.): McGraw-Hill International Book Company, 1988.
- Saracco, G., Geobaldo, F., and Baldi, G., "Methane combustion on Mg-doped LaMnO_3 perovskite catalysts", *Appl. Catal. B*, 1999, **20**, 277-288.
- Satterfield, C. N., *Heterogeneous Catalysis in Industrial Practice: Heterogeneous Catalytic Oxidation*, (n.p.): McGraw-Hill, 1980.
- Spivey, J.J., "Complete Oxidation of Volatile Organics", *Ind. Eng. Chem.Res.*, 1987, **26**, 2165-2180.
- Thammanokul, H., "Oxidative dehydrogenation of propane over V-Mg-O catalysts", *Master's Thesis, Faculty of Engineering, Chulalongkorn University*, 1996.
- The JCPDS., *Inorganic Phases Alphabetical Index*, 1980.
- Tongsang, P., "The application of V-Mg-O/ TiO_2 catalyst on the combustion of anhydrides", *Master's Thesis, Faculty of Engineering, Chulalongkorn University*, 2001.
- Toyada, Y., and Teraji, S., "Process for the treatment of byproducts obtained in the preparation of phthalic anhydride" *United States Patent*, 1980, **4181489**, 1-18.
- Umpo, S., "The application of Co-Mg-O/ Al_2O_3 catalyst on the combustion of anhydrides", *Master's Thesis, Faculty of Engineering, Chulalongkorn University*, 2001.
- Vassileva, M., Andreev, A., Dancheva, S., and Kotsev, N., "Complete catalytic oxidation of benzene over supported vanadium oxides modified by palladium", *Appl. Catal.*, 1989, **49**, 125-141.
- Wachs, I.E., Saleh, R.Y., Chan, S.S., and Chersich, C.C., "The interaction of vanadium pentoxide with titania (anatase)", *Appl. Catal.*, 1985, **15**, 339-352.
- Way, T., and Peter, F., "Apparatus for the recovery of vaporized phthalic anhydride from gas streams" *United States Patent*, 1981, **4252772**, 1-20.

Weng, R.Y., and Lee, J.F., "Catalytic performance and active sites determination of niobium oxide promoted vanadium / titania catalysts for selective catalytic reduction of nitric oxide" *Appl. Catal.*, 1993, **105**, 41-51.

Yao, Y.F.U., "Catalytic oxidation of Ethanol at Low Concentrations" *Ind. Eng. Chem. Process Des. Dev.*, 1984, **23**, 60-67.



สถาบันวิทยบริการ
จุฬาลงกรณ์มหาวิทยาลัย



APPENDICES

สถาบันวิทยบริการ
จุฬาลงกรณ์มหาวิทยาลัย

APPENDIX A

CALCULATION OF CATALYST PREPARATION

Preparation of 8Cu-7V-1Mg-O/ TiO₂ catalysts by the Wet Impregnation Method is shown as follow:

Reagent:	- Cupric nitrate trihydrate(CuN ₂ O ₆ ·3H ₂ O) Molecular weight = 241.60 g.
	- Magnesium nitrate [Mg(NO ₃) ₂] Molecular weight = 256.41 g.
	- Ammonium metavanadate [NH ₄ (VO ₃)] Molecular weight = 116.98 g
Support	- Titania [TiO ₂]

Calculation for the preparation of the 8Cu-7V₂O₅-1Mg-O/TiO₂ catalyst.

The 8Cu-7V₂O₅-1Mg-O/TiO₂ aqueous solution used in catalyst preparation consists of V₂O₅ 7wt% and TiO₂ 93wt%. The amounts of copper and magnesium in 8Cu-7V₂O₅ -1Mg-O/ TiO₂ catalyst are calculated as follows:

Preparation of :7V₂O₅/TiO₂ 5 g

If the weight of catalyst was 100 g, 7V₂O₅/TiO₂ would compose of V₂O₅ 7 g and TiO₂ 93 g. Therefore, in this system,

$$\begin{aligned} \text{the amount of V}_2\text{O}_5 &= 7/100 \times 5 \\ &= 0.35 \text{ g} \end{aligned}$$

Vanadia (V₂O₅) 0.35 g was prepared from NH₄(VO₃) and molecular weight of V₂O₅ = 181.88 , then

$$\begin{aligned} \text{the amount of content NH}_4(\text{VO}_3) \text{ used} & \\ &= (116.98/181.88) \times 0.35 \\ &= 0.4502 \text{ g} \end{aligned}$$

Thus

$$\begin{aligned} \text{The amount of TiO}_2 &= 5 - 0.35 \\ &= 4.65 \text{ g} \end{aligned}$$

basis : $7\text{V}_2\text{O}_5/\text{TiO}_2$ 5 g

Then, the Cu: (support + V_2O_5) weight ratio = 8:92

$$\begin{aligned} \text{The amount of Cu} &= 8/92 \times 5 \\ &= 0.4348 \text{ g} \end{aligned}$$

Copper (Cu) 0.4348 g was impregnated from $(\text{CuN}_2\text{O}_6 \cdot 3\text{H}_2\text{O})$ solution and molecular weight of Cu = 63.546 g

$$\begin{aligned} \text{the amount of } (\text{CuN}_2\text{O}_6 \cdot 3\text{H}_2\text{O}) \text{ used} &= (0.4348 \times 241.60) / (63.546) \\ &= 1.6531 \text{ g} \end{aligned}$$

and the Mg: ($7\text{V}_2\text{O}_5/\text{TiO}_2$ + Cu) weight ratio = 1:100

$$\begin{aligned} \text{The amount of Mg} &= (5 + 0.4348) \times 1/100 \\ &= 0.0543 \text{ g} \end{aligned}$$

Magnesium (Mg) 0.0543 g was impregnated from $\text{Mg}(\text{NO}_3)_2$ solution 99% and molecular weight of Mg = 24.305 g

$$\begin{aligned} \text{Thus, the amount of } \text{Mg}(\text{NO}_3)_2 \text{ used} &= (0.0543 \times 256.41 \times 100) / (24.305 \times 99) \\ &= 0.5791 \text{ g} \end{aligned}$$

The calculation for the preparation of other catalysts as follow $8\text{Fe}-7\text{V}_2\text{O}_5-1\text{Mg}-\text{O}/\text{TiO}_2$, $8\text{Mo}-7\text{V}_2\text{O}_5-1\text{Mg}-\text{O}/\text{TiO}_2$ and $8\text{Zn}-7\text{V}_2\text{O}_5-1\text{Mg}-\text{O}/\text{TiO}_2$ catalysts were the same as the preparation of $8\text{Cu}-7\text{V}_2\text{O}_5-1\text{Mg}-\text{O}/\text{TiO}_2$ catalysts.

APPENDIX B

CALCULATION OF DIFFUSIONAL LIMITATION EFFECT

In the present work there are doubt whether the external and internal diffusion limitations interfere with the phthalic anhydride combustion reaction. Hence, the kinetic parameters were calculated based on the experimental data so as to prove the controlled system. The calculation is divided into two parts; one of which is the external diffusion limitation, and the other is the internal diffusion limitation.

1. External diffusion limitation

The phthalic anhydride combustion reaction is considered to be an irreversible first order reaction occurred on the interior pore surface of catalyst particles in a fixed bed reactor. Assume isothermal operation for the reaction.

In the experiment, 0.01% phthalic anhydride, 21% O₂ was used as the unique reactant in the system. Because percentage of phthalic anhydride was rather small compared to the oxygen that it can be neglected. Molecular weight of nitrogen and oxygen are 28.02 and 31.98, respectively. Thus, the average molecular weight of the gas mixture was calculated as follows:

$$\begin{aligned}M_{AB} &= 0.79 \times 28.02 + 0.21 \times 31.98 \\ &= 28.85 \text{ g/mol}\end{aligned}$$

Calculation of reactant gas density

Consider the phthalic anhydride combustion is operated at low pressure and high temperature(500°C). We assume that the gases are respect to ideal gas law. The density (ρ) of such gas mixture reactant at various temperatures (T) is calculated in the following.

$$\rho = PM / RT$$

where ρ = gas density
 M = molecular weight
 R = gas constant
 T = absolute temperature

We obtained : $\rho = 0.455 \text{ kg/m}^3$

Calculation of the gas mixture viscosity

The simplified methods for determining the viscosity of low pressure binary are described elsewhere (Reid, 1988). The method of Wilke is chosen to estimate the gas mixture viscosity.

For a binary system of 1 and 2,

$$\mu_m = \frac{y_1 \mu_1}{y_1 + y_2 \Phi_{12}} + \frac{y_2 \mu_2}{y_2 + y_1 \Phi_{21}}$$

where μ_m = viscosity of the mixture
 μ_1, μ_2 = pure component viscosity
 y_1, y_2 = mole fractions

$$\phi_{12} = \frac{\left[1 + \left(\frac{\mu_1}{\mu_2} \right)^{1/2} \left(\frac{M_1}{M_2} \right)^{1/4} \right]^2}{\left[8 \left(1 + \frac{M_1}{M_2} \right) \right]^{1/2}}$$

$$\phi_{21} = \phi_{12} \left(\frac{\mu_2}{\mu_1} \right) \left(\frac{M_1}{M_2} \right)$$

M_1, M_2 = molecular weight

Let 1 refer to nitrogen and 2 to oxygen

$$M_1 = 28.02 \text{ and } M_2 = 31.98$$

From Perry (1973) the viscosity of nitrogen at 500°C are 0.0368 cP. The viscosity of oxygen at 500°C are 0.039cP.

$$\phi_{12} = 0.971$$

$$\phi_{21} = 0.902$$

$$\mu_m = 3.81 \times 10^{-5} \text{ kg/m-s}$$

Calculation of diffusion coefficients

Diffusion coefficients for binary gas system at low pressure calculated by empirical correlation are proposed by Reid (1988). Wilke and Lee method is chosen to estimate the value of D_{AB} due to the general and reliable method. The empirical correlation is

$$D_{AB} = \frac{\left(3.03 - \frac{0.98}{M_{AB}^{1/2}}\right) (10^{-3}) T^{3/2}}{PM_{AB}^{1/2} \sigma_{AB}^2 \Omega_D}$$

where D_{AB} = binary diffusion coefficient, cm^2/s

T = temperature, K

M_A, M_B = molecular weights of A and B, g/mol

$$M_{AB} = 2 \left[\left(\frac{1}{M_A} \right) + \left(\frac{1}{M_B} \right) \right]^{-1}$$

P = pressure, bar

σ = characteristic length, Å

Ω_D = diffusion collision integral, dimensionless

The characteristic Lennard-Jones energy and length, ε and σ , of nitrogen and oxygen are as follows: (Reid,1988)

For O_2 : $\sigma = 3.467 \text{ \AA}$, $\varepsilon/k = 106.7$

For N_2 : $\sigma = 3.798 \text{ \AA}$, $\varepsilon/k = 71.4$

The sample rules are usually employed.

$$\sigma_{AB} = \frac{\sigma_A + \sigma_B}{2} = \frac{3.798 + 3.467}{2} = 3.63$$

$$\varepsilon_{AB}/k = \left(\frac{\varepsilon_A \varepsilon_B}{k^2} \right)^{1/2} = (71.4 \times 106.7)^{1/2} = 87.28$$

Ω_D is tabulated as a function of kT/ε for the Lennard-Jones potential. The accurate relation is

$$\Omega_D = \frac{A}{(T^*)^B} + \frac{C}{\exp(DT^*)} + \frac{E}{\exp(FT^*)} + \frac{G}{\exp(HT^*)}$$

where $T^* = \frac{kT}{\varepsilon_{AB}}$, $A = 1.06036$, $B = 0.15610$, $C = 0.19300$, $D = 0.47635$, $E = 1.03587$, $F = 1.52996$, $G = 1.76474$, $H = 3.89411$

Then $T^* = 8.857$

$$\Omega_D = \frac{1.06036}{(T^*)^{0.15610}} + \frac{0.19300}{\exp(0.47635T^*)} + \frac{1.03587}{\exp(1.52996T^*)} + \frac{1.76474}{\exp(3.89411T^*)}$$

$$\Omega_D = 0.757$$

With Equation of D_{AB} ,

$$D(N_2-O_2) = 1.123 \text{ m}^2/\text{s}$$

Reactant gas mixture was supplied at 100 ml/min. in tubular microreactor used in the phthalic anhydride oxidation system at 30°C

air flow rate through reactor = 100 ml/min. at 30°C

The density of air , $\rho = 1.161 \text{ kg/m}^3$

Mass flow rate = $1.935 \times 10^{-6} \text{ kg/s}$

Diameter of stainless steel tube reactor = 9.5 mm

Cross-sectional area of tube reactor = $\frac{\pi(9.5 \times 10^{-3})^2}{4} = 7.09 \times 10^{-5} \text{ m}^2$

Mass Velocity , $G = 0.027 \text{ kg/m}^2\text{-s}$

Catalyst size = 40-60 mesh = 0.178-0.126 mm

Average catalyst size = $(0.126+0.178)/2 = 0.152 \text{ mm}$

Find Reynolds number, Re_p , which is well known as follows:

$$Re_p = \frac{d_p G}{\mu}$$

We obtained

$$Re_p = 0.108$$

Average transport coefficient between the bulk stream and particles surface could be correlated in terms of dimensionless groups, which characterize the flow conditions. For mass transfer the Sherwood number, $k_m \rho / G$, is an empirical function of the Reynolds number, $d_p G / \mu$, and the Schmit number, $\mu / \rho D$. The j-factors are defined as the following functions of the Schmidt number and Sherwood numbers:

$$j_D = \frac{k_m \rho}{G} \left(\frac{a_m}{a_t} \right) (\mu / \rho D)^{2/3}$$

The ratio (a_m/a_t) allows for the possibility that the effective mass-transfer area a_m , may be less than the total external area, a_t , of the particles. For Reynolds number greater than 10, the following relationship between j_D and the Reynolds number well represents available data.

$$j_D = \frac{0.458}{\varepsilon_B} \left(\frac{d_p G}{\mu} \right)^{-0.407}$$

where G = mass velocity(superficial) based upon cross-sectional area of empty reactor

$$(G = u\rho)$$

d_p = diameter of catalyst particle for spheres

μ = viscosity of fluid

ρ = density of fluid

ε_B = void fraction of the interparticle space (void fraction of the bed)

D = molecular diffusivity of component being transferred

Assume $\varepsilon_B = 0.5$

$$j_D = 2.266$$

A variation of the fixed bed reactor is an assembly of screens or gauze of catalytic solid over which the reacting fluid flows. Data on mass transfer from single screens has been reported by Gay and Maughan. Their correlation is of the form

$$j_D = (\varepsilon k_m \rho / G)(\mu / \rho D)^{2/3}$$

Where ε is the porosity of the single screen.

$$\text{Hence, } k_m = (j_D G / \rho)(\mu / \rho D)^{-2/3}$$

$$k_m = \left(\frac{0.458G}{\varepsilon_B \rho} \right) \text{Re}^{-0.407} \text{Sc}^{-2/3}$$

$$\text{Find Schmidt number, Sc : } \text{Sc} = \frac{\mu}{\rho D}$$

$$\text{Sc} = 7.456 \times 10^{-5}$$

$$\text{Find } k_m : \quad k_m = 75.90 \text{ m/s}$$

Properties of catalyst

Density = 0.375 g/ml catalyst

Diameter of 40-60 mesh catalyst particle = 0.152 mm

$$\text{Weight per catalyst particle} = \frac{\pi(0.152 \times 10^{-1})^3 \times 0.375}{6} = 6.895 \times 10^{-7} \text{ g/particle}$$

External surface area per particle = $\pi(0.152 \times 10^{-3})^2 = 7.26 \times 10^{-8} \text{ m}^2/\text{particle}$

$$a_m = (7.26 \times 10^{-8}) / (6.895 \times 10^{-7}) = 0.105 \text{ m}^2/\text{gram catalyst}$$

Volumetric flow rate of gaseous feed stream = 100 ml/min

Molar flow rate of gaseous feed stream = $6.71 \times 10^{-5} \text{ mol/s}$

Phthalic anhydride molar feed rate = $0.0001 \times 6.71 \times 10^{-5} = 6.71 \times 10^{-9} \text{ mol/s}$

phthalic anhydride conversion (experimental data): 99.80% at 500°C

The estimated rate of phthalic anhydride oxidation reaction is based on the ideal plug flow reactor which there is no mixing in the direction of flow and complete mixing perpendicular to the direction of flow (i.e., in the radial direction). The rate of reaction will vary with reaction length. Plug flow reactors are normally operated at steady state so that properties at any position are constant with respect to time. The mass balance around plug flow reactor becomes



$$\begin{aligned} & \{\text{rate of } i \text{ into volume element}\} - \{\text{rate of } i \text{ out of volume element}\} \\ & + \{\text{rate of production of } i \text{ within the volume element}\} \\ & = \{\text{rate of accumulation of } i \text{ within the volume element}\} \end{aligned}$$

$$\begin{aligned} F_{A_0} &= F_{A_0}(1-x) + (r_W W) \\ (r_W W) &= F_{A_0} - F_{A_0}(1-x) = F_{A_0} x = F_{A_0} X \end{aligned}$$

$$r_W = \frac{F_{A_0} X}{W} = 6.70 \times 10^{-10} \text{ mol/s-gram catalyst}$$

At steady state the external transport rate may be written in terms of the diffusion rate from the bulk gas to the surface. The expression is:

$$\begin{aligned} R_{\text{obs}} &= k_m a_m (C_b - C_s) \\ &= \frac{\text{phthalic anhydride converted (mole)}}{(\text{time})(\text{gram of catalyst})} \end{aligned}$$

where C_b and C_s are the concentrations in the bulk gas and at the surface, respectively.

$$(C_b - C_s) = \frac{r_{\text{obs}}}{k_m a_m} = 8.407 \times 10^{-11} \text{ mol/m}^3$$

Consider the difference of the bulk and surface concentration is small. It means that the external mass transport has no effect on the phthalic anhydride oxidation reaction rate.

2. Internal diffusion limitation

Next, consider the internal diffusion limitation of the phthalic anhydride reaction. An effectiveness factor, η , was defined in order to express the rate of reaction for the whole catalyst pellet, r_p , in terms of the temperature and concentrations existing at the outer surface as follows:

$$\eta = \frac{\text{actual rate of whole pellet}}{\text{rate evaluated at outer surface conditions}} = \frac{r_p}{r_s}$$

The equation for the local rate (per unit mass of catalyst) may be expected functionally as $r = f(C, T)$.

Where C represents, symbolically, the concentrations of all the involved components

Then, $r_p = \eta r_s = \eta f(C_s, T_s)$

Suppose that the phthalic anhydride oxidation is an irreversible reaction $A \rightarrow B$ and first order reaction, so that for isothermal conditions $r = f(C_A) = k_1 C_A$. Then $r_p = \eta k_1 (C_A)_s$.

For a spherical pellet, a mass balance over the spherical-shell volume of thickness Δr . At steady state the rate of diffusion into the element less the rate of diffusion out will equal the rate of disappearance of reactant within the element. This rate will be $\rho_p k_1 C_A$ per unit volume, where ρ_p is the density of the pellet. Hence, the balance may be written, omitting subscript A on C,

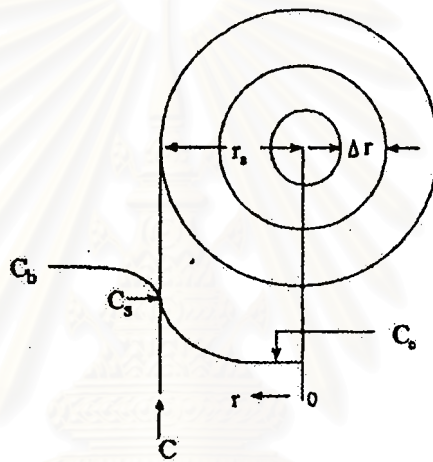


Figure B1. Reactant (A) concentration vs. position for first-order reaction on a spherical catalyst pellet.

$$\left(-4\pi r^2 D_e \frac{dC}{dr} \right)_r - \left(-4\pi r^2 D_e \frac{dC}{dr} \right)_{r+\Delta r} = -4\pi r^2 \Delta r_p k_1 C$$

Take the limit as $\Delta r \rightarrow 0$ and assume that the effective diffusivity is independent of the concentration of reactant, this difference equation becomes

$$\frac{d^2 C}{dr^2} + 2 \frac{dC}{dr} - \frac{k_1 \rho_p C}{D_e} = 0$$

At the center of the pellet symmetry requires

$$\frac{dC}{dr} = 0 \text{ at } r = 0$$

and at outer surface

$$C = C_s \text{ at } r = r_s$$

Solve linear differential equation by conventional methods to yield

$$\frac{C}{C_s} = \frac{r_s \sinh\left(3\phi_s \frac{r}{r_s}\right)}{r \sinh 3\phi_s}$$

where ϕ_s is Thiele modulus for a spherical pellet defined by $\phi_s = \frac{r_s}{3} \sqrt{\frac{k_1 \rho_p}{D_e}}$

Both D_e and k_1 are necessary to use $r_p = \eta k_1 (C_A)_s$. D_e could be obtained from the reduced pore volume equation in case of no tortuosity factor.

$$D_e = (\epsilon_s^2 D_{AB})$$

$$D_e = (0.5)^2 (1.123) = 0.281$$

Substitute radius of catalyst pellet, $r_s = 7.6 \times 10^{-5}$ m with ϕ_s equation

$$\phi_s = 9.253 \times 10^{-7} \sqrt{k} \text{ (dimensionless)}$$

Find k (at 500°C) from the mass balance equation around plug-flow reactor.

$$r_w = \frac{F_{A0} dx}{dW}$$

where $r_w = kC_A$

$$\text{Thus, } kC_A = \frac{F_{A0} dx}{dW}$$

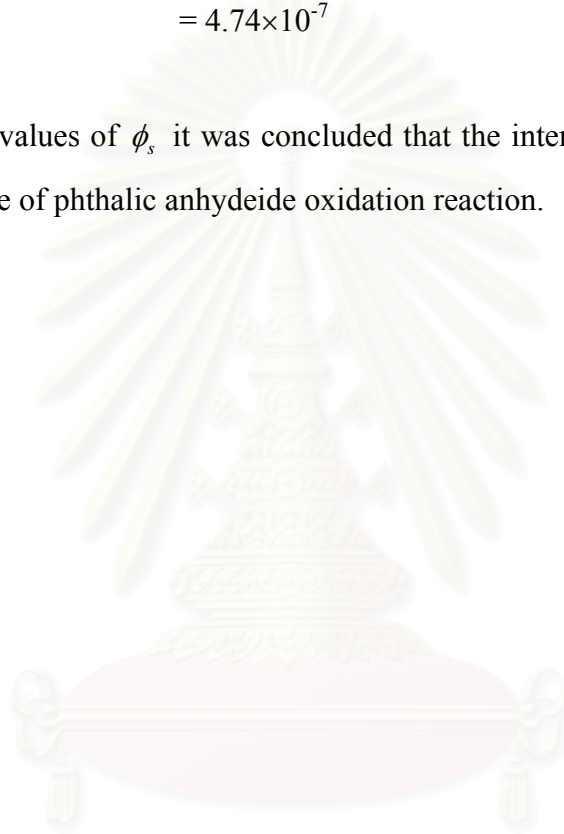
$$kC_{A_0}(1-x) = \frac{F_{A_0} dx}{dW}$$

$$W = \frac{F_{A_0}}{kC_{A_0}} \int_0^{0.998} \frac{1}{1-x} dx$$

$$k = 0.262 \text{ m}^3/\text{s}\cdot\text{kg catalyst}$$

$$\begin{aligned} \text{Calculate } \phi_s : \phi_s &= 9.253 \times 10^{-7} \sqrt{0.262} \\ &= 4.74 \times 10^{-7} \end{aligned}$$

For such small values of ϕ_s it was concluded that the internal mass transport has no effect on the rate of phthalic anhydride oxidation reaction.



สถาบันวิทยบริการ
จุฬาลงกรณ์มหาวิทยาลัย

APPENDIX C

CALCULATION OF SPECIFIC SURFACE AREA

From Brunauer-Emmett-Teller (BET) equation [Anderson and co-worker (1985)]

$$\frac{p}{n(1-p)} = \frac{1}{n_m C} + \frac{(C-1)p}{n_m C} \quad (C1)$$

Where, p = Relative partial pressure of adsorbed gas, P/P_0
 P_0 = Saturated vapor pressure of adsorbed gas in the condensed state at the experimental temperature, atm
 P = Equilibrium vapor pressure of adsorbed gas, atm
 n = Gas adsorbed at pressure P , ml. at the NTP/g of sample
 n_m = Gas adsorbed at monolayer, ml. at the NTP/g of sample
 C = $\text{Exp} [(H_C - H_1)/RT]$
 H_C = Heat of condensation of adsorbed gas on all other layers
 H_1 = Heat of adsorption into the first layer

For the single point method, the graph must pass through the origin. Therefore, the value of C must be assumed to be infinity.

$C \rightarrow \infty$, then equation C1 is reduced to

$$\frac{p}{n(1-p)} = \frac{p}{n_m}$$
$$n_m = n(1-p) \quad (C2)$$

The surface area, S , of the catalyst is given by

$$S = S_b \times n_m \quad (C3)$$

From the gas law

$$\frac{P_b V}{T_b} = \frac{P_t V}{T_t} \quad (C4)$$

Where, P_b = Pressure at 0°C
 P_t = Pressure at $t^\circ\text{C}$
 T_b = Temperature at $0^\circ\text{C} = 273.15 \text{ K}$

T_t = Temperature at $t^\circ\text{C}$ = $273.15 + t$ K

V = Constant volume

Then, $P_b = (273.15 / T_t) \times P_t = 1$ atm

Partial pressure

$$p = \frac{[\text{Flow of (He + N}_2) - \text{Flow of He}]}{\text{Flow of (He + N}_2)} \quad (\text{C5})$$

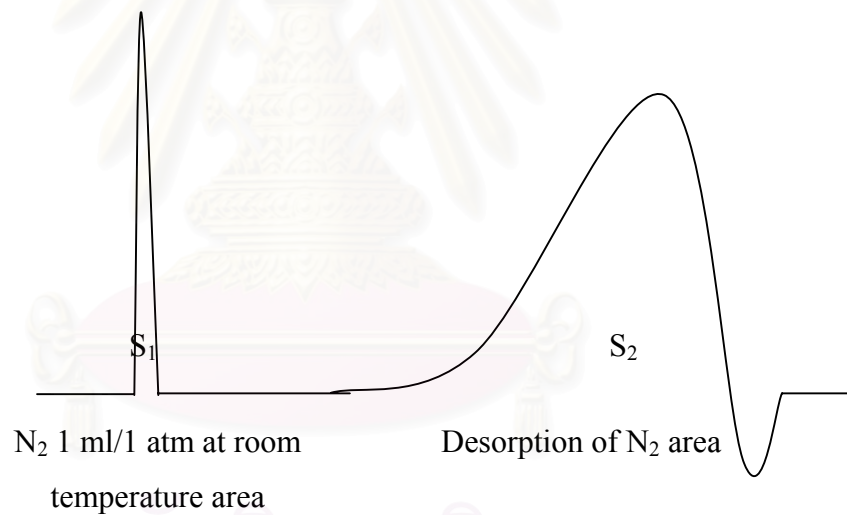
$$= 0.3 \text{ atm}$$

For nitrogen gas, the saturated vapor pressure equals to

$P_0 = 1.1$ atm

then, $p = P/P_0 = 0.3/1.1 = 0.2727$

To measure the volume of nitrogen adsorbed, n



$$n = \frac{S_2}{S_1} \times \frac{1}{W} \times \frac{273.15}{T} \text{ ml/g of catalyst} \quad (\text{C6})$$

Where, S_1 = N_2 1 ml/1 atm at room temperature area

S_2 = Desorption of N_2 area

W = Sample weight, g

T = Room temperature, K

Therefore,

$$n_m = \frac{S_2}{S_1} \times \frac{1}{W} \times \frac{273.15}{T} \times (1-p)$$

$$n_m = \frac{S_2}{S_1} \times \frac{1}{W} \times \frac{273.15}{T} \times 0.7272 \quad (C2.1)$$

Whereas, the surface area of nitrogen gas from literature equal to

$$S_b = 4.373 \text{ m}^2/\text{ml of nitrogen gas}$$

Then,

$$S = \frac{S_2}{S_1} \times \frac{1}{W} \times \frac{273.15}{T} \times 0.7272 \times 4.343$$

$$S = \frac{S_2}{S_1} \times \frac{1}{W} \times \frac{273.15}{T} \times 3.1582 \text{ m}^2/\text{g} \quad (C7)$$

สถาบันวิทยบริการ
จุฬาลงกรณ์มหาวิทยาลัย

APPENDIX D

CALIBRATION CURVES

Flame ionization detector gas chromatographs Shimadzu model 9A equipped with a Chromosorb WAW column is used to analyze the concentrations of phthalic anhydride.

The Porapak-Q and Molecular Sieve 5-A column are used with a gas chromatograph equipped with a thermal conductivity detector, Shimadzu model 8A, to analyze the concentration of CO₂ and CO.

The calibration curves of phthalic anhydride and carbon dioxide are illustrated in the following figures.



สถาบันวิทยบริการ
จุฬาลงกรณ์มหาวิทยาลัย

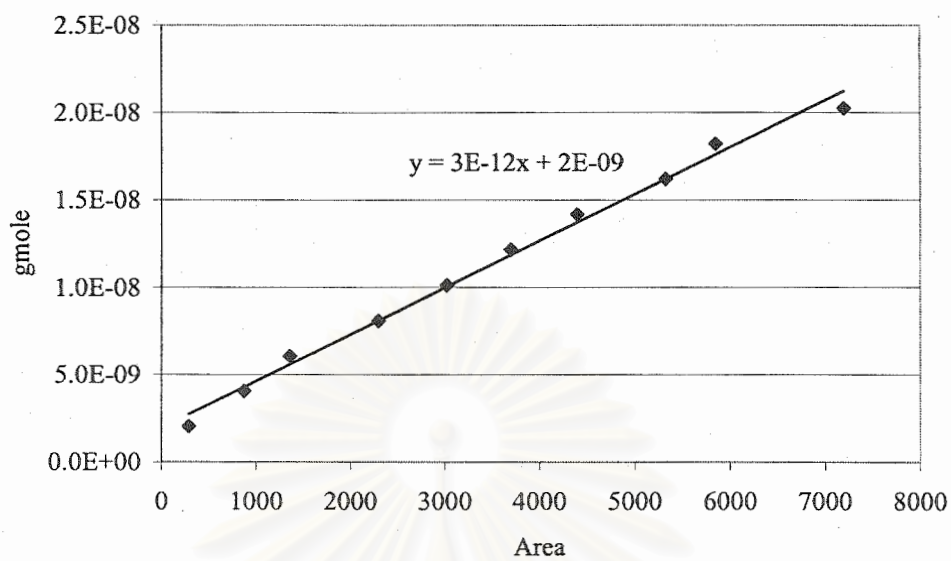


Figure D1 The calibration curve of phthalic anhydride

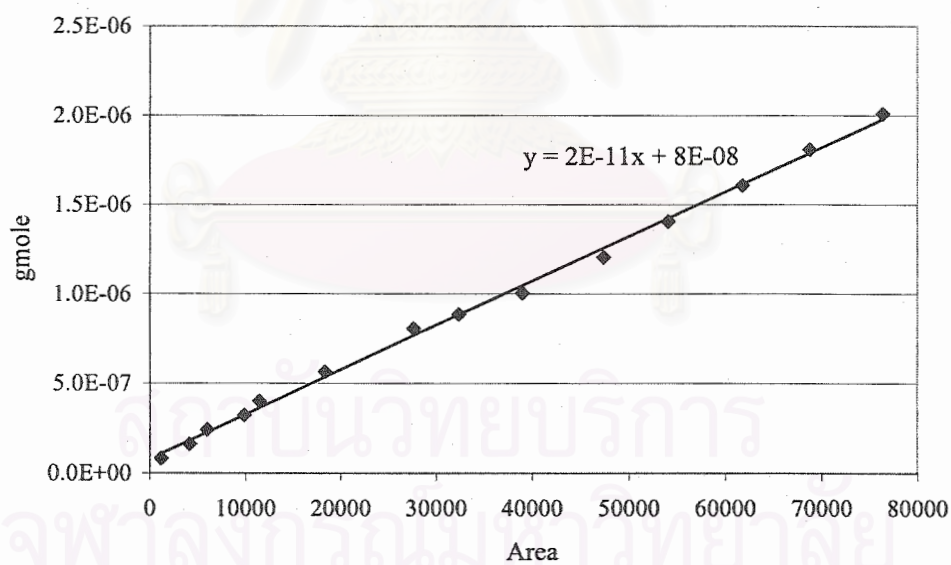


Figure D2 The calibration curve of carbon dioxide

APPENDIX E

DATA OF EXPERIMENTS

Table E1 Data of [Figure 5.2 to 5.5](#)

Temp (°C)	Phthalic anhydride conversion (%)	
	Cu-V-Mg-O/TiO ₂	Fe-V-Mg-O/TiO ₂
200	3.00	2.70
250	33.00	16.50
280	60.00	37.00
300	76.00	55.00
350	81.00	73.00
400	83.00	82.00
450	89.00	91.00
500	95.00	93.00

Table E1 Data of [Figure 5.2 to 5.5](#)

Temp (°C)	Phthalic anhydride conversion (%)	
	Zn-V-Mg-O/TiO ₂	Mo-V-Mg-O/TiO ₂
200	5.00	8.00
250	54.00	16.50
280	62.00	35.00
300	69.00	45.00
350	73.00	63.00
400	80.00	78.00
450	90.00	89.00
500	91.00	93.50

Table E1 Data of [Figure 5.2 to 5.5](#)

Temp (°C)	Phthalic anhydride conversion (%)
	V ₂ O ₅ /TiO ₂
200	1.00
250	12.00
280	13.00
300	15.00
350	30.00
400	50.00
450	90.00
500	91.00

Table E2 Data of pyridine and maleic anhydride adsorption of [Table 5.3](#)

Metal	Pyridine adsorption	Maleic anhydride adsorption
TiO ₂	15006849	1590170
V ₂ O ₅ /TiO ₂	6226498	1480021
Cu-V-Mg-O/TiO ₂	2566777	1675645
Fe-V-Mg-O/TiO ₂	3114910	1823418
Mo-V-Mg-O/TiO ₂	5824161	2761236
Zn-V-Mg-O/TiO ₂	4185471	1371055



สถาบันวิทยบริการ
จุฬาลงกรณ์มหาวิทยาลัย

APPENDIX F

MATERIAL SAFETY DATA SHEETS

Phthalic anhydride

Safety data for phthalic anhydride

General

Synonyms: 1,2-benzenedicarboxylic acid anhydride, phthalic acid anhydride

Molecular formula: $C_8H_4O_3$

Physical data

Appearance: white crystalline solid with choking odor

Melting point: $131^{\circ}C$

Boiling point: $295^{\circ}C$

Vapour density: 5.1 (air=1)

Density ($g\ cm^{-1}$): 1.53

Flash point: $152^{\circ}C$ (closed cup)

Explosion limit: 1.7-10.5%

Water solubility: slight

Stability

Stable. Combustible. Incompatible with strong oxidizing agents, strong bases, moisture, nitric acid, alkalis. Dust may form an explosive mixture with air.

Toxicology

Corrosive - causes burns. Harmful if swallowed or inhaled. Skin or eye contact may cause severe irritation. Typical TLV/TWA 1 ppm. Typical STEL 4 ppm. Typical PEL 2 ppm.

Personal protection

Safety glasses, gloves, adequate ventilation.



สถาบันวิทยบริการ
จุฬาลงกรณ์มหาวิทยาลัย

APPENDIX G

PROCEDURE AND CALCULATION OF PYRIDINE AND MALEIC ANHYDRIDE ADSORPTION

Pyridine Adsorption

The nitrogen gas flowed through the system that consisted of a tube connected to the gas chromatograph (GC9A). The sample was placed in the tube as shown in Figure G1.

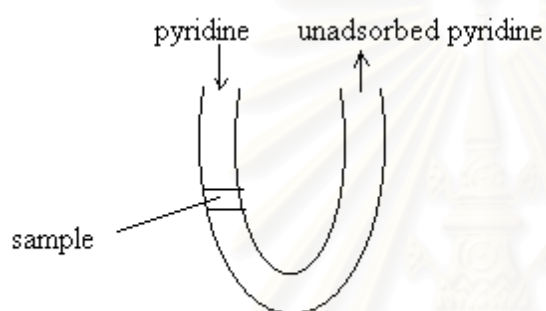


Figure G1 The adsorption system

The pyridine was injected into the column. The sample would adsorb a part of the pyridine. The pyridine that was not adsorbed on the sample was measured by the gas chromatograph. The pyridine was injected until the peaks were constant. It meant that the sample was saturated with pyridine.

The peaks of the unadsorbed pyridine that were detected from the gas chromatograph were shown in Figure G2.

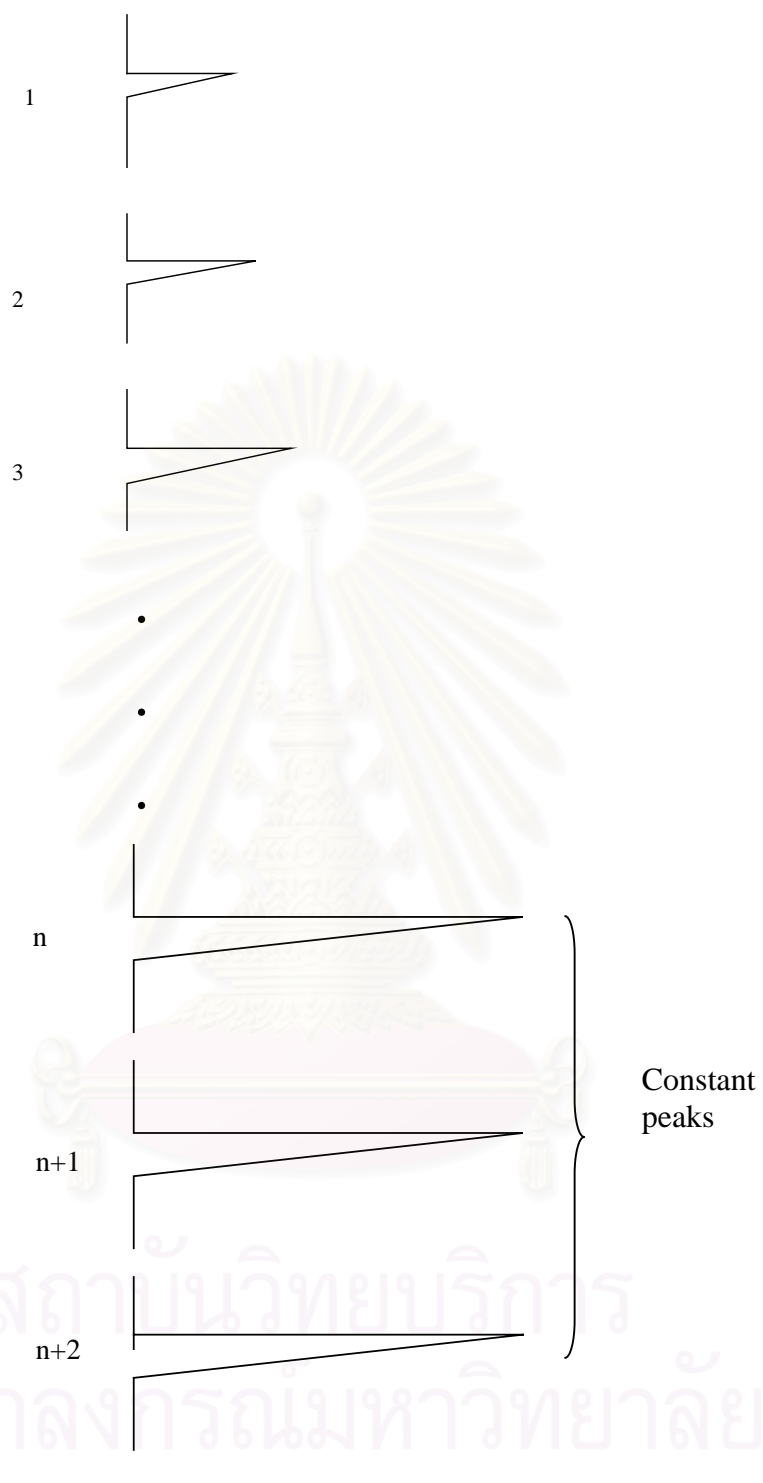


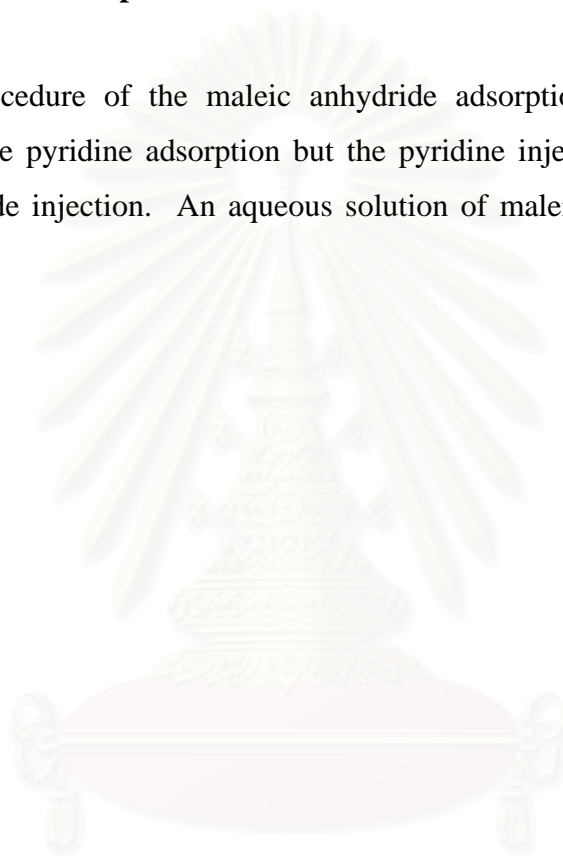
Figure G2 The unadsorbed pyridine peaks

The overall pyridine adsorbed was calculated by subtraction the area of constant peaks with the 1st peak, 2nd peak, ..., respectively. The summation of these subtracted areas was the overall area of the pyridine adsorbed.

$$\text{Overall pyridine adsorbed} = \sum (\text{area of constant peak} - \text{area of peak}_i)$$

Maleic anhydride adsorption

The procedure of the maleic anhydride adsorption was the same as the procedure of the pyridine adsorption but the pyridine injection was changed to the maleic anhydride injection. An aqueous solution of maleic anhydride (0.104 g/ml) was used.



สถาบันวิทยบริการ
จุฬาลงกรณ์มหาวิทยาลัย

VITA

Miss Nalinpan Charoenruay was born on January 18th, 1981 in Bangkok, Thailand. She received the Bachelor Degree of Chemical Engineering from Faculty of Engineering, Chulalongkorn University in 2002. She continued her Master's Study at Chulalongkorn University in June, 2002.



สถาบันวิทยบริการ
จุฬาลงกรณ์มหาวิทยาลัย